Journal of Archaeological Method and Theory
https://doi.org/10.1007/s10816-022-09584-4

# Life Around the Elephant in Space and Time: an Integrated Approach to Study the Human-Elephant Interactions at the Late Lower Paleolithic Site of La Polledrara di Cecanibbio (Rome, Italy)

**Cristina Lemorini[1] · Ernesto Santucci[2] · Isabella Caricola[1] · Alessandro Nucara[3] · Stella Nunziante-Cesaro[4]**

Accepted: 27 September 2022


## Abstract

During the Lower Paleolithic, the interaction between hominins and elephants through the medium of lithic tools is testified by numerous sites in Africa, Europe, and Asia. This interaction ensured hominins a large source of food and of knappable raw material, bone. The availability of the huge package of resources represented by these animals had a deep impact on hominins behavior and their strategies of exploitation of the landscape. This article, for the first time, documents this behavior with a spatial and chronological viewpoint. At the Late Lower Paleolithic site of La Polledrara di Cecanibbio (Rome), the outstanding in situ find of a quite entire carcass of *Palaeoloxodon antiquus* surrounded by lithic tools of small dimensions allowed us to explore the relation between the elephant, fatally entrapped in muddy sediments, and the hominins that exploited its carcass with their lithic toolkit. The application of an integrated approach including technology, refitting, use-wear, residues, and spatial analyses to the study of the small tools allowed us to unveil the activities carried out around the elephant in a timeline. As a result, hominins exploited the carcass for meat and fat possibly in more than one time and selected the area of the carcass as an atelier to knap and possibly cache their lithic products for future use. These data introduce the intriguing suggestion that the carcass was, besides a source of food and raw material, also a landmark for humans in the landscape.

**Keywords** Megafauna · Hominins · Late Lower Paleolithic · Small tools · Time · Space · Integrated approach

✉ Cristina Lemorini
cristina.lemorini@uniroma1.it

Extended author information available on the last page of the article

Published online: 24 October 2022

## Introduction

The interaction between hominins and elephants during the Lower Paleolithic is testified by numerous sites in Africa, Europe, and Asia where remains of *Palaeoloxodon antiquus* and lithic tools coexist (see Agam & Barkai, 2018; Panagopoulou *et al*., 2018 and refs therein). The presence of anthropogenic bone surface modifications (BSMs) on elephant bones is powerful direct evidence of this interaction (Haynes & Krasinski, 2021; Solodenko *et al*., 2015; Tourloukis *et al*., 2018) through the medium of lithic tools. In addition to these data, the presence of lithic tools with residues and use-wear related to the processing of animal tissues (skin, meat, bone) near elephant carcasses (Mosquera *et al*., 2015; Solodenko *et al*., 2015; Aranguren *et al*., 2019) reinforces the involvement of these animals in the diet of hominins in the Lower Paleolithic.

Elephants were a source of meat, fat, and marrow, which are all very suitable high-energy foods (Ben-Dor *et al*., 2011; Reshef & Barkai, 2015). Elephant bones were also exploited as raw material to produce flakes and various types of large tools among which handaxes are the most iconic (Zutovski & Barkai, 2016; Barkai, 2021; Villa *et al*., 2021).

In addition to all the data and the arguments in favor of the interaction between hominins and elephants, the enormous importance of these animals as sources of food and raw material surely had a deep impact on hominins behavior and their strategies of exploitation of the landscape. These strategies may have consisted of the organization of a hunting session, or the exploitation of a carcass encountered during the routine exploration and exploitation of the landscape. It is highly probable that, in the case of the encounter with a carcass and depending on its state of preservation—intact, partly scavenged by other predators, totally scavenged—the potential of exploitation differed and, thus, hominins probably adopted a certain flexibility in their behavior and their toolkit to take advantage of these situations. Behavioral flexibility implies cognitive mechanisms that allow the proper toolkit to be "put into use" when the "target," the elephant, materializes in one of the possible conditions (prey to be hunted, carcass to be exploited). Surely, flakes and retouched flakes of small size, also known as small flakes and small tools, were part of this toolkit (see Pargeter and Shea (2019) for a review of miniaturization in lithic technology). These items, generally not exceeding the 4-cm maximum length (Starkovich *et al*., 2021 p.3), are found, from Oldowan onward, in contexts where elephant remains are present (see Abruzzese *et al*., 2016; Tourloukis *et al*., 2018; Marinelli *et al*., 2021a and refs. therein). Moreover, their link with elephant carcasses is confirmed by their spatial correlation with elephant carcasses in various contexts (Aureli *et al*., 2015; Santucci *et al*., 2016; Tourloukis *et al*., 2018 and refs therein), correlation which is also confirmed by the use-wear analysis (Mosquera *et al*., 2015; Santucci *et al*., 2016). Small tools are the ideal toolkit of mobile communities for their portability associated with their cutting efficiency, as tested in various controlled experiments (Chazan, 2013; Key & Lycett, 2015; Marinelli *et al*., 2021b). Among them, the experiment conducted by Starkovich *et al*. (2021) proved their effectiveness in processing an elephant limb.

The detailed analysis of the strategies adopted and the appreciation of eventually distinct episodes of interaction between hominins and elephants are possible in contexts where the formation of the anthropic layers was fast and any or minimal episodes of disturbance occurred.

The Late Lower Paleolithic site of La Polledrara di Cecanibbio (Rome, Italy) is one of the few archaeological contexts that show these ideal conditions (Santucci *et al*., 2016 and refs therein).

Here we present the results of an integrated approach combining refitting, technological, use-wear, residues, and spatial analyses of the lithic tools related to the exploitation of the carcass, quite entirely in anatomical connection, of an elephant. Technological and, especially, refitting analyses (see also Mosquera *et al*., 2015; Aureli *et al*., 2015) combined with the spatial analysis were crucial to appreciate at a precise scale when distinct episodes of knapping occurred and where they occurred. Moreover, the integration of the spatial analysis with the refitting, the use-wear, and the residue analyses allowed us to document the processing of the carcass with the lithic tools, to investigate their spatial connection with the carcass, and to understand if and how these tools originated from knapping episodes in situ.

Furthermore, this integrated study allowed us to investigate the functional role of toolkits of small size to exploit elephant carcasses. At La Polledrara, the lithic assemblage is represented by flint tools of small size only. The connection between small size tools, butchering activities, and elephant was already documented by previous use-wear analysis (Santucci *et al*., 2016). With this paper, we further reveal the interaction of hominins, small tools, and elephants at a spatial and temporal scale.

## Materials and Methods

### The Archaeological Context

The Pleistocene deposit of La Polledrara di Cecanibbio (Rome) is located in the most southern offshoot of the Sabatino volcanic system. The deposit was discovered in 1984 and excavated for more than 30 years; a substantial part of the exposed paleosoil (900m$^2$) is now open to the public as a permanent museum (Santucci *et al*., 2016). A fluvio-palustrine system originated the deposit (Anzidei *et al*., 2012; Santucci *et al*., 2016 Fig. 2 p. 172) at the beginning of MIS 9 (Milli & Palombo, 2005; Milli *et al*., 2008), as confirmed by $^{40}$Ar/$^{39}$Ar radiometric dating of 325–310 ka (Pereira *et al*., 2017).

The deposit is the result of various episodes of transportation and accumulation of volcanoclastic sediments (Castorina *et al*., 2015) due to fluvial, at first, and then palustrine events (Anzidei *et al*., 2012; Santucci *et al*., 2016). In the first fluvial stage, numerous remains of fauna were transported and accumulated during flood episodes. Then, the progressive infilling of the paleo river created areas of waterlogging characterized by thick layers of thin sediments subjected to cycles of soaking, drying, and, probably, rearrangement. In the layers corresponding to the palustrine phases, remains of three carcasses of *Palaeoloxodon antiquus* were found in

the distinct areas of the site. The three carcasses were positioned at very different heights, probably depending on the shape of the underlying riverbed.

The lack of several portions of the two of them is probably due to various factors: localized episodes of water flow that incised and cleared away the mud, possible anthropic manipulation of the portions of the carcasses, and modern field work due to agriculture.

The third carcass, excavated during the years 2006–2014, is quite complete except for a few lacking bones composing the hip girdle, ribs, and the vertebral column (Fig. 1a, b). The great interest of these remains is due, in addition to the exceptional degree of preservation and entirety, to their association with numerous lithic tools, partially knapped and used *in loco*. The results of the research presented here refer to this context.

The elephant remains are distributed in a space of approximately 25m$^2$ in the northeast area of the deposit. They are related to an adult, probably a male, entrapped in muddy sediments during the palustrine phase of the deposit (Santucci

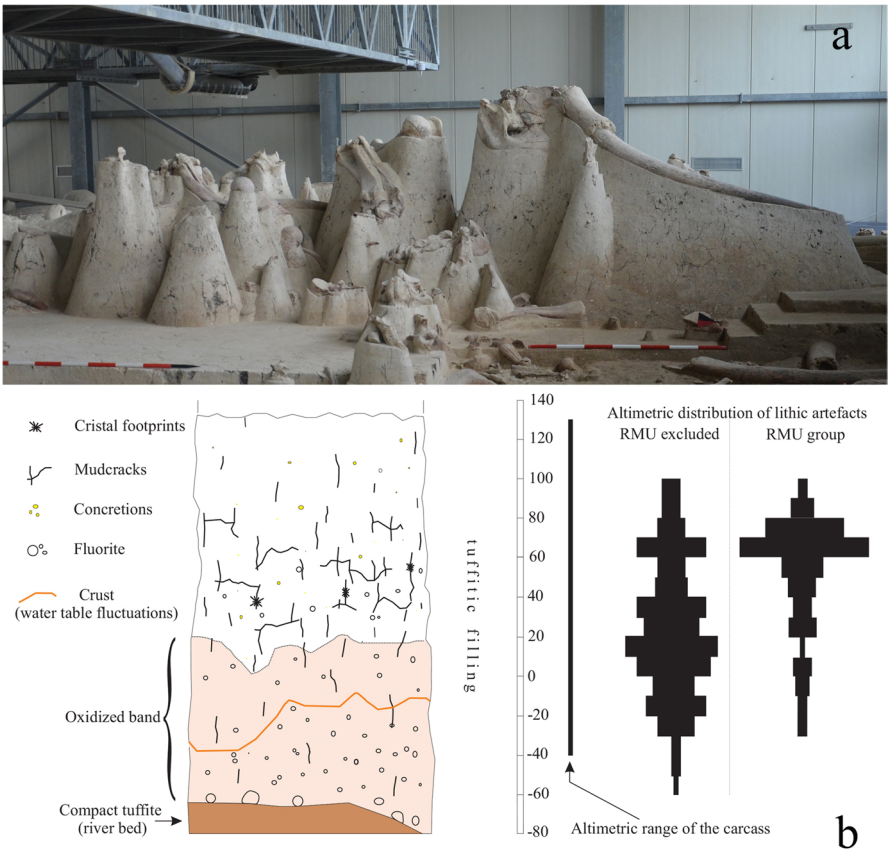


**Fig. 1** The Palaeoloxodon carcass from the east (**a**); stratigraphy of the carcass area with altimetry of the carcass bulk and the distribution of the lithic industry (**b**)

*et al*., 2016, Fig. 1 p. 171, Figs. 3, 4, and 5, pp. 173–174). The posture of the limbs and the morphology of the paleoriver suggest that the elephant, coming from the south, sank into a depression filled with soaked and plastic tuffite (Fig. 2). Its position, slightly reclined on the left side with the left posterior limb stretch, testifies to the final disarranged attempt to advance, no longer able to control its descent with the usual and correct position elephants exhibit, with the posterior limbs flexed and the anterior limbs stretched (see Gröning and Saller (2000) for a similar situation documented in the wild).

The carcass lies with the four limbs in anatomical connection. The proximal ends of the femurs are missing, due to intentional anthropic breakage (Cerilli & Fiore,

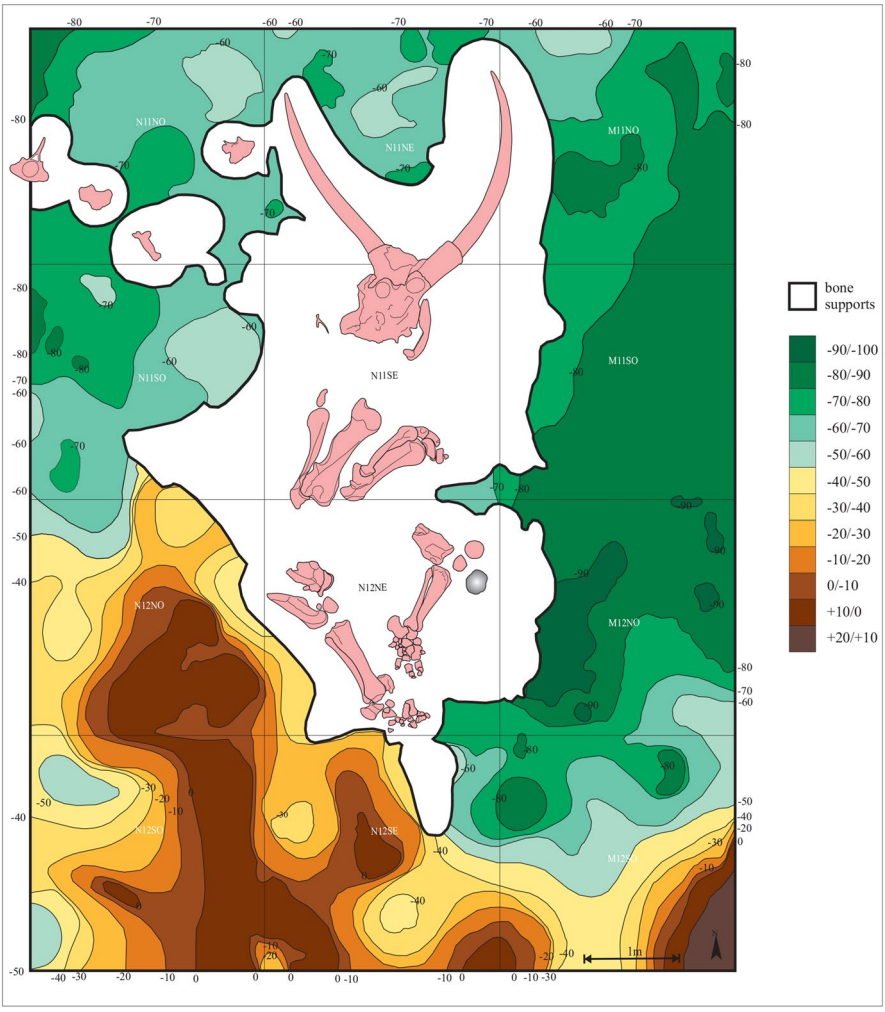


**Fig. 2** Bottom morphology around the carcass (compact tuffite of the paleo-river bed). Isoipse at intervals of 10 cm indicated by the chromatic scale on the right (higher elevation in shades of brown)

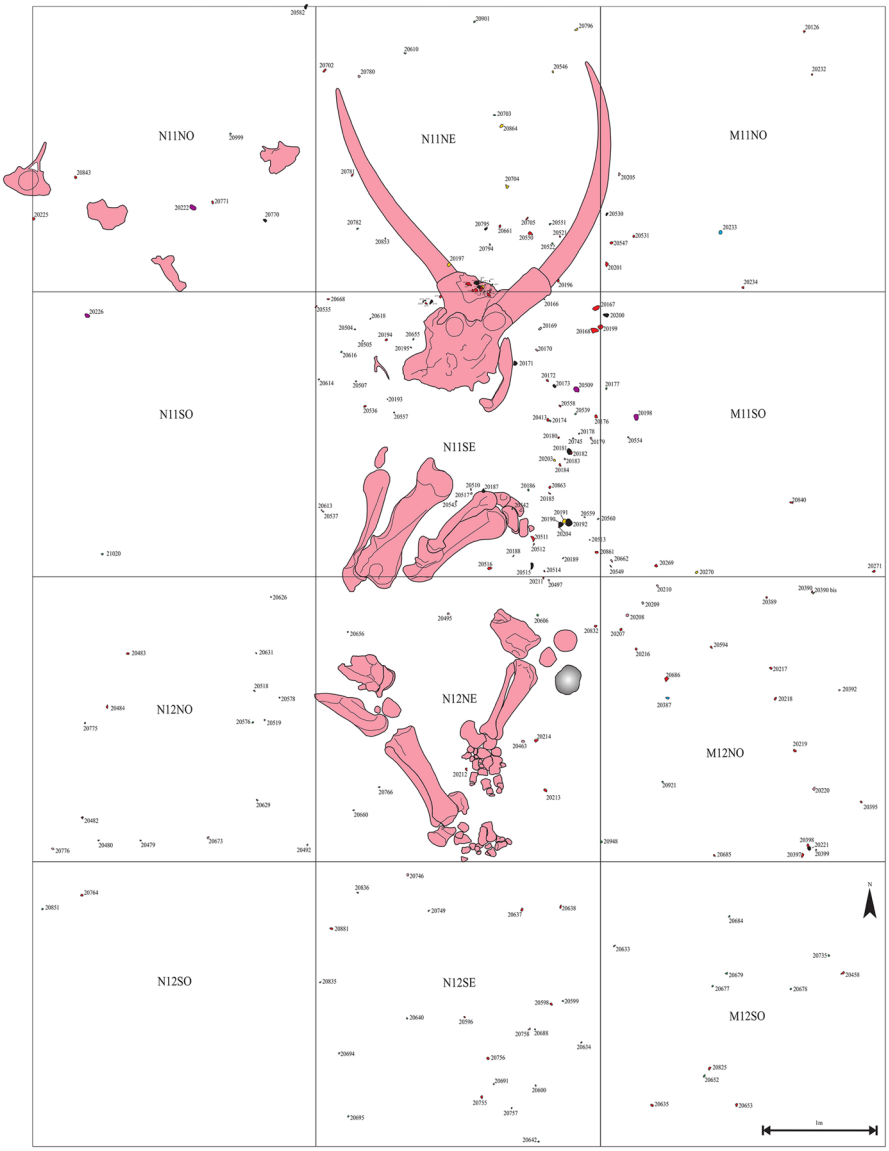


**Fig. 3** General distribution of lithic implements in the carcass area (plan)

2018). The humerus, rib cage, and scapulae are also missing. In this case, it is not possible to recognize the precise cause of this absence. Although there are no stratigraphic elements in favor of postdepositional events, the lack of these anatomic part of the carcass can be associated with multiple factors, including human and animal factors (see White and Diedrich (2012) and refs therein for neo-taphonomic processes). The skull is almost intact, and the jaw and the tusks are still in place. The

hyoid bone, one rib, and several cervical vertebrae, the latter lying west of the skull, are also present.

Other elephant bones, located in the same area at lower altitudes, do not pertain to the main carcass. Other remains are distributed on the tuffite surface of the paleo riverbed; their sedimentary position and their poor preservation suggest that their transportation was due to a high energy fluvial phase, at the beginning of the sedimentary accumulation of the deposit.

## The Lithic Assemblage

The lithic assemblage is distributed around the elephant carcass at a linear distance not exceeding 4 m; the area occupied by the elephant (approximately 33 $m^2$) plus the lithic industry measures approximately 75 $m^2$ (Fig. 3). No other fauna has been documented in this area except for a few fragments pertaining to *Bos primigenius*. The borders of the area coincide with the borders of the squares where the lithic items were found. The thickness of the excavated tuffite layers has a high variation, between 1 and 2 m, due to the morphology of the paleo riverbank.

The majority of the debitage, raw material (pebbles), and cores was found during the excavation and positioned on the excavation grid. Conversely, most of the microlithic component consisting of waste, fragments, and indeterminable items was found during the sieving activity performed on the entire volume of the excavated deposit with a sieve with a fine mesh of 1 mm (Table 1). It is worth mentioning that possibly few lithic artifacts pertaining to the area of the elephant may still be buried on the columns of deposit that allow the maintenance of the carcass in place for the need of museum display (Santucci *et al*., 2016, Fig. 3, p. 174).

## Site Formation Processes and Degree of Preservation of the Lithic Tools

The site formation processes that occurred in the osseous remains of La Polledrara were recently discussed in Marano *et al*. (2021). The paper focuses on the fauna accumulated on the bend of a paleoriver excavated in the basal tuffite deposit. X-ray fluorescence spectroscopy, Fourier-transform infrared spectroscopy (FTIR), and scanning electron microscopy-energy-dispersive x-ray (SEM–EDX) analyses were applied to characterize the mineralogical composition of the deposit and the fauna. As a result, accretions of barite were detected forming tabular elongated crystals. These crystals filled the inner voids of the bones as well as their external surface. Marano et al. suggested that the

**Table 1** Lithic items found in the area of the elephant

| | Pebbles/ cores/flakes | Waste/fragments/ indet. pieces | Total |
|---|---|---|---|
| Items positioned on the grid | 151 | 72 | 223 |
| Items from sieving | 10 | 383 | 393 |
| Total | 161 | 455 | 616 |

migration of the barite is probably due to successive sequences of soaking of the deposit by ground water surfacing and by humidity that these bones are still exposed to in the current public exhibit.

The preliminary macroscopic observation of the lithic assemblage found in the area of the elephant suggested that the stone tools underwent very few if any alterations. This consideration was partly confirmed by the observation of the lithic surfaces at the low magnification with a reflected light system. No mechanical stress, such as edge damage, fractures, or abrasions, was detected; however, spots of very thin encrustation with a white-yellowish granular appearance were visible on the surface of most of the lithic tools (Fig. 4a, b). The observation at higher magnification with a metallographic microscope and a reflected light system confirmed the presence of a very thin crust (Fig. 4c) partly sealing the surface of the tools.

This crust had a white-fluorescent appearance in the SEM observation (Fig. 4d) and the EDX elemental analysis allowed us to detect the high presence of sulfur (S) and barium (Ba) (SI Fig. S1a; SI Table S1), which testifies to the production of crystals of barite (barium sulfate $BaSO_4$), similar to what was detected by Marano *et al*. (2021). These accretions overlap a thin blackish deposit mostly composed of silicon (Si) and aluminum (Al) with the addition of iron (Fe) and calcium (Ca) in minor quantities (SI Fig.S1b; SI Table S1). This elemental composition suggests that the phase of precipitation of $BaSO_4$ followed the deposition of a thin layer of sandy clay.

FTIR analysis of the surface of the lithic tools could not have contributed to the detection of barite residues since the most intense vibrational modes of this compound (Bahl *et al*., 2014 and refs therein) fall in the same spectroscopic region of the silicon oxide stretching modes of flint.

Similar to the lithics, we detected the barite on fragments of fauna found in the same area near the elephant.

SEM–EDX observation of the internal surface of the fragments revealed that barite also partly filled the voids forming oriented tabular elongated crystals comparable to those observed by Marano *et al*. (2021) (Fig. 4e; SI Fig. S1c).

Additionally, in this case, infrared spectroscopic analysis of bone samples could not support the existence of barite remains since phosphor-calcium of apatite (Habuda-Stanić *et al*., 2014) and sulfur-oxygen of barite stretching modes fall in the same frequency range.

The accretion of barite associated with lithics and fauna from the elephant area may indicate the soaking of the mud where the elephant was entrapped with ground waters enriched in the ions Ba + and SO =. The presence of the water was also indicated by diatoms entrapped in the barite and in its substratum (Fig. 1f). It appears that the process that caused barite accretion in the elephant area was less pronounced than that in the paleoriver area (Marano *et al*., 2021). The accretion observed on the lithic tools and on the fauna consisted of a thin layer of barite originating from a few fast sequences of precipitation. Probably, after the soaking event, the area was affected by a long time-lapse of desiccation that allowed to seal the deposit, favoring the post-depositional preservation of the lithic tools.

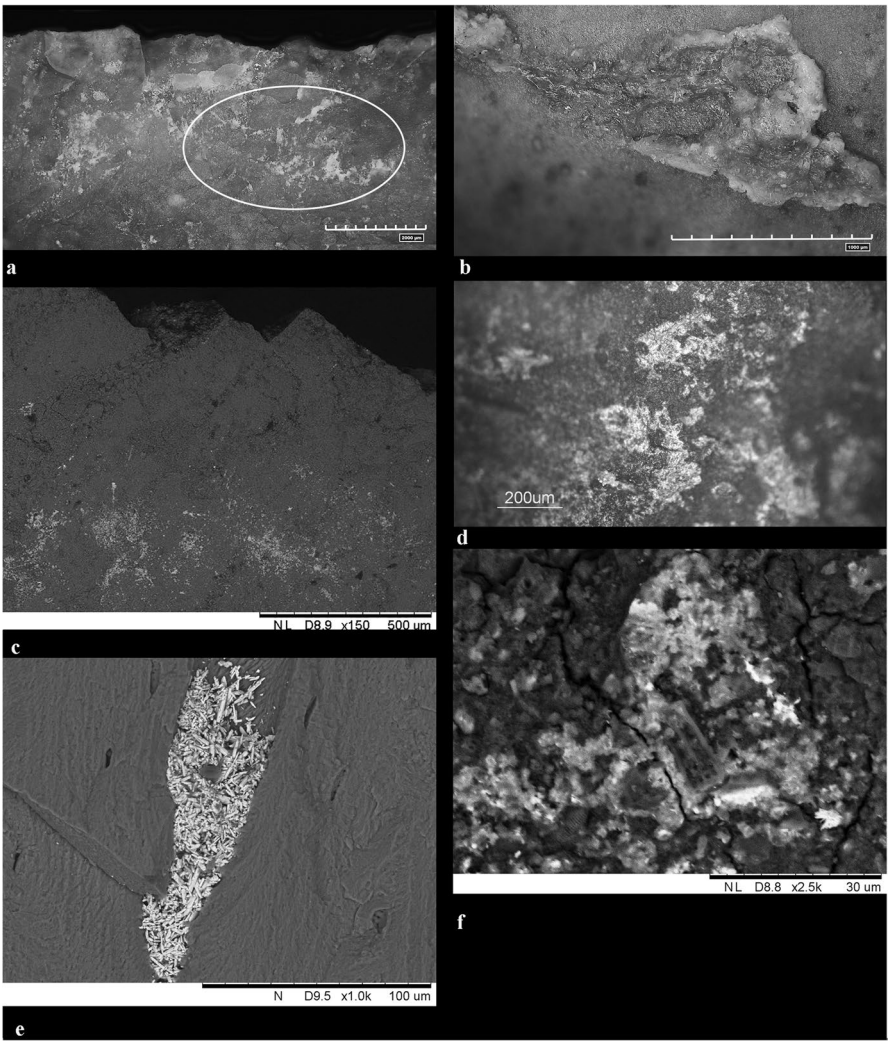


**Fig. 4** Spots of encrustation observed on the lithic tools. Encrustation appearance by OLM observation (**a**, **b**, **d**); encrustation appearance by SEM observation (**c**); crystal formation on the micro-cavity of the bone remains detected by SEM (**e**); diatoms deposited on the encrustation detected by SEM (**f**)

## Cleaning Procedure

In many cases, the accretions observed on the lithic tools made difficult the observation of the underlying surface and, as a consequence, the observation of residues and use-wear; thus, it was decided to gently remove the aggregates with a few minutes of washing with ultra-pure water in an ultrasonic tank. Due to the soft procedure, the residues deeply entrapped in the lithic surface and the

adipocere, a waxy waterproof substance derived from the transformation of fat acids, were not affected by the cleaning procedure.

The removal of the crystals revealed a well-preserved surface suggesting that the encrustation did not activate processes of patination, but rather probably contributed to avoiding its development.

All items were manipulated with powder-free gloves, during cleaning and during all the steps of the analysis. Once residues were analyzed, the archaeological items were washed in preparation for the use-wear analysis. The archaeological items were initially washed with tap water, and subsequently treated in a bath of ultra-pure water with a 2% solution of buffered soap Derquim (Asryan et al., 2014). The items were then treated in an ultrasonic tank for 5 min, followed by a final rinsing using ultra-pure water in an ultrasonic tank for 5 min.

### Technological and Refitting Analyses and Spatial Analysis

Flakes and cores were analyzed to document all the features of their surface useful to reconstruct the strategies and the techniques applied to produce the lithic industry of La Polledrara (Boëda *et al*., 1990; Inizan *et al*., 1995): striking platform (morphology, extent, angle) and surfaces of detachment (direction, syntax, and sequence of the detachments) on cores; butts, ventral surface features (bulb, profile, termination), and dorsal surface features (cortex presence and position, direction, syntax, and sequence of the negatives) on flakes. Diacritical schemes were produced for each lithic item except for the debris.

Refitting analysis was a primary source of direct inference of the reduction methods, the organization of the space, and the identification of the postdepositional disturbances (Romagnoli & Vaquero, 2019). The macroscopic analysis of the raw materials and the detection of blanks with analogous texture and similar chromatic associations of the cortex, of the subcortical area, if present, and of the inner surface allowed us to identify the raw material units (RMUs) (Roebroeks, 1988).

The estimation of the usable blanks and the missing blanks was tentatively carried out for the RMUs that included cores.

Areas with a different density of artifacts, intuitively observed on the planimetry, were confirmed by 2D statistical analysis (i.e., kernel density). However, the depositional context and the extent of its volumes made it essential to consider the third dimension ($z$-axis).

Clusters and dispersions were investigated by calculating the proximity index between the lithic tools. The position of the items pertaining to the RMUs and their links added important data for the comprehension of anthropic contributions to site formation (Cziesla, 1990).

## Residues Analysis

### Morphological Analysis and SEM–EDX Analysis

Observation of the lithic items was performed using the low- and high-magnification approaches (Hayes & Rots, 2019) by means of an RH-Hirox digital microscope (magnifications up to 1000×) and a Hitachi Tabletop TM3000 SEM (magnification up to 5000×, observation standard mode total vacuum, observation condition 15 kV). The investigation continued with the sampling of the microresidues, taken from the surface of the stone tools using a precision graduated sterile pipette and ultra-pure water. The samples were placed on a slide and observed with the addition of Picro-Sirius Red stain solution (ab246832®) useful for the identification of collagen, following the protocol published by Stephenson (2015). Finally, the slides were observed using a Nikon Eclipse metallographic microscope with polarized and transmitted light, with a magnification range between 50× and 200×.

The organic residues were compared with an experimental reference collection (Caricola *et al*., 2022), in addition to those known in the literature (Fullagar *et al*., 2017; Hayes & Rots, 2019; Lombard & Wadley, 2007; Pedergnana *et al*., 2016; Pedergnana & Ollé, 2018; Pedergnana, 2020; Wadley *et al*., 2004; Martín-Viveros & Ollé, 2020; Venditti *et al*., 2021a, b).

### FTIR-PCA

Infrared spectra of the residues were acquired with a Bruker FTIR instrument (Bruker Alpha R) equipped with an accessory for the reflectance measurements not requiring previous treatment of the sample. The area analyzed had a diameter of approximately 3 mm. The spectra were obtained by collecting 50 to 200 scans and had a resolution of 4 $cm^{-1}$. As spectral artifacts can be generated by environmental contamination of the lithic residues (Frahm *et al*., 2022), all the precautions have been taken during the laboratory work and FTIR experiments have also been performed on possible contaminants to evaluate their occurrence in the spectra of the residues.

Principal components analysis (PCA) of the infrared data was performed according to the procedure reported in Caporaletti *et al*. (2017). The matrix of the absorption intensities (matrix dimension $N \times M$, with $N$ = number of spectra and $M$ = number of data points) was processed with commercial and in-house codes, all based on NIPALS algorithms (Wright, 2017).

### Use-Wear Analysis

Use-wear analysis was conducted by combining low- and high-power approaches by a Nikon SMZ stereomicroscope with a magnification up to 7.5×, Nikon Eclipse metallurgical microscope with a magnification up to 500× and RH-Hirox digital microscope with magnification up to 1000× (Lemorini *et al*., 2020 and refs. therein).

The low-power approach was useful for obtaining a broad view of the localization of the use-traces on the tool, and it was useful for observing and describing edge rounding and edge removals. The high-power approach was useful for observing microwear, such as polishes and striation along with microrounding of the edge.

## Results

### Technological and Refitting Analyses

In the area of the elephant, 616 lithic artifact (Table 2) mostly consisting of small fragments and debris (2/3 of the whole assemblage, followed by cores, flakes, and retouched flakes) were collected and analyzed. This assemblage did not include lithic showing alteration due to weathering or high energy river flow. Their heavy patination strongly differed from the high degree of preservation of most of the lithic artifact, suggesting their intrusive origin in the context.

The lithic industry was entirely produced with siliceous pebbles (SI Fig.S2) from the Ponte Galeria Formation (Funiciello *et al*., 2008). The maximum size of the pebbles ranges from 5 to 7 cm with some few exceptions reaching a maximum 8.5 cm. The texture of the flint is mostly fine-grained (95%). Some pebbles show cleavage plane fractures that, nevertheless, did not prevent their exploitation.

The technological features observed on the lithic items suggested the predominant use of the direct percussion technique with a hard hammer (pronounced bulbs, large butts, absence of a lip on the proximal ventral surface) and a poor control of the percussion (incipient cones inside the residual striking platform, hinge or step fracture, siret accident). The features that qualitatively characterize the bipolar

**Table 2** Composition of the lithic assemblage found in the area of the elephant

| Exploitable blanks | |
|---|---|
| Pebbles and pebbles fragments | 4 |
| Cores on pebble and related fragments | 15 |
| Core on flakes | 11 |
| Cores and cores fragments on indet. blanks | 3 |
| Indeterminable blanks | 2 |
| Flakes undamaged | 84 |
| Flakes fragments | 20 |
| Indeterminable flakes fragments | 22 |
| Total | 161 |
| Waste | |
| MFL max dim. < 15 mm, l + w ≥ 19 mm | 74 |
| MFM max dim. < 15 mm, l + w ≥ 11 mm ≤ 18 mm | 129 |
| MFS max dim. < 15 mm, l + w ≤ 10 mm | 73 |
| Fragments | 104 |
| Indeterminable | 75 |
| Total | 455 |

technique (opposite bulbs or negative, opposite battering scars or blunt edge) (de la Peña, 2015; Pargeter & Eren, 2017) are present at La Polledrara in one case only. Nevertheless, a small group of flakes (9% of the whole assemblage) show transversal marked furrows on the proximal ventral surface similar to dihedral negative or the presence of flat or slightly concave ventral surfaces without bulbs and marked concentric undulations. These features suggest the possible presence of the bipolar technique carried out on the ground or using an osseous surface as anvil instead of the stone split fracture technique (Crabtree, 1972; Faivre *et al*., 2011).

Among the 616 lithic artifact pertaining to the elephant area, 29 are cores and 126 flakes and flake fragments with dimensions and morphology suitable for use (flakes unretouched and retouched, flake fragments). The minimum dimension of the potentially functional blanks ($\geq$ 1.5 cm) was fixed on the bases of the smallest entire artifact with use-wear. Microflakes compose 276 items, divided into three dimensional subgroups: large microflakes (MFL), medium microflakes, and small microflakes (Table 2). These microflakes originated from the retouching activity and, mostly, by failed flake extractions, secondary flakes, and écaillures.

There are also 104 fragments of flakes and 75 indeterminate fragments including two entire pebbles and a third one broken in half along a cleavage plane. No hammerstones were recognized.

### Cores (Fig. 5)

There are 14 cores on pebbles. One of them (ID 20221) is a core on a pebble deeply exploited and then slightly retouched on its overhang to create an edge used to scrape bone (see the "Use-Wear Analysis" section).

The production sequences are quite simple. The selected pebbles are slightly flat thus already set for the extraction of the flakes without preliminary shaping and without the preparation of the striking platform. The latter is mostly cortical and extended from 25 to 50% of the entire perimeter of the pebble. The flaking angles range from 55° to 70°.

Generally, the flake scars are distributed on one or two surfaces of debitage along the third dimension of the pebble (thickness). The prevailing technique is unidirectional and more rarely convergent (Table 3).

In the convergent system, the secondary flaked surface possibly alternate with the primary surface; more often, they are independent. An average of four flake scars $\geq$ 15 mm was observed on the residual primary flaked surface. The average diminished to three flake scars on the secondary flaked surface if present.

The cores on flake number 11; they vary from thick flakes with multiple detachments to thin flakes with one or two detachments. They were exploited with unidirectional and, more often, convergent systems.

Two multifaceted cores were also identified, one on the pebble and one on the core on flake. The other three cores were totally exploited, and the original blank is unidentifiable.

The cores show different stages and different strategies of exploitation. In some cases, large pebbles were minimally exploited by a single detachment; in contrast,

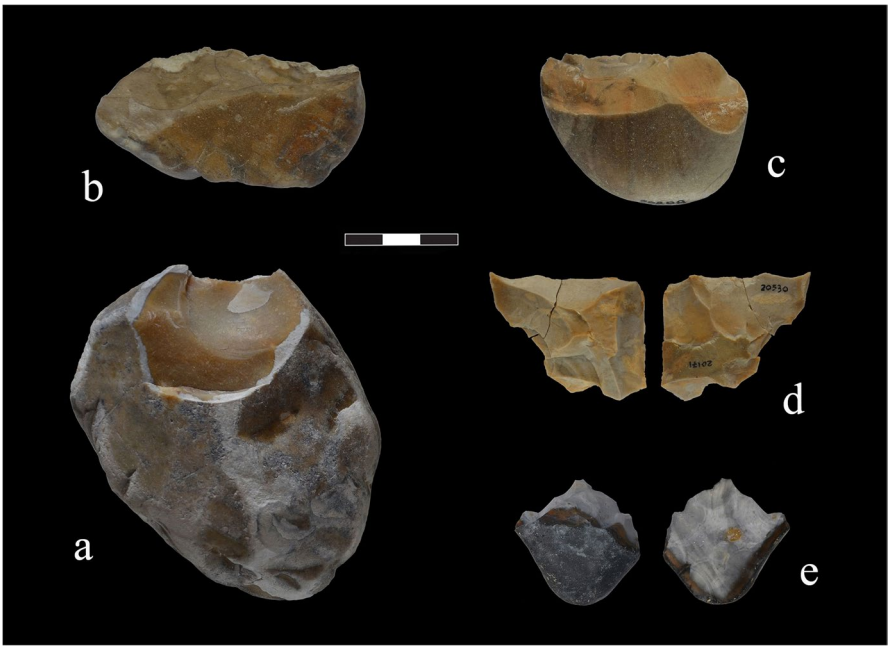


**Fig. 5** Sample of lithic industry. Cores. Unidirectional reduction on pebbles (one flaking surface and natural striking platform) (a–c); core on pebble with two flaking surfaces (mixed syntax with unidirectional and converging series) (d); unidirectional reduction on flake (striking platform on ventral surface of the flake) (e)

**Table 3** Technological features of the lithic assemblage; *U* unidirectional, *C* convergent, *I* indeterminable

| No | Blank | 1 flaking surface | | 2 flaking surfaces | | | | >2 flaking surface |
|---|---|---|---|---|---|---|---|---|
| | | U | C | U+U | U+C | C+C | C+I | |
| 14 | Pebble | 8 | – | 2 | 1 | 1 | – | 1 |
| 11 | Flake | 4 | 3 | – | 1 | – | 1 | 1 |
| 3 | Indet | – | 1 | – | – | – | 1 | - |

raw material with internal cleavage planes was heavily exploited and show various flake scars.

## The Debitage (Fig. 6)

The debitage consists of 126 flakes (Table 2). The total number of undamaged flakes is 84 and their maximal length and maximal width, except for a few cases, do not exceed 4 cm × 3 cm.

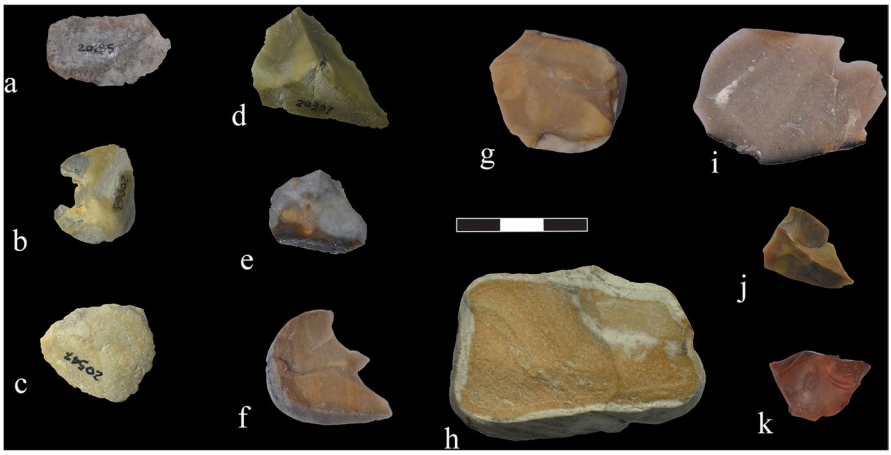


**Fig. 6** Sample of lithic industry. Flakes at different stage of the reduction. Total cortex (a–c); distal cortex (d–e); natural backs (segments) (f–g); peripheral cortex (slice) (h); absent cortex (i–k)

The cortex is present on 70% of the flakes; among this group, 29% are full cortical flakes, and 71% are partly cortical in their lateral or distal-lateral area. The 19% of the flakes were the result of the initial blow to open the pebble or the result of the preparation of the flaked surface.

The negative scars ≥ 15 mm on the dorsal surface of the flakes number generally one or two, rarely three. Their unidirectional orientation prevails similar to the case of the cores.

Six other flakes show residual ventral surfaces on their dorsal side; they were all knapped from cores on flakes. Most likely, they represent the accidental byproduct of production sequences aimed continuing to exploit cores with an already reduced volume. Ninety-four butts and 93 bulbs were identified. The butts are mostly cortical (74%), more rarely flat (14%), linear (7%), and scaled (5%). The bulbs are mostly simple (69%). Multiple bulbs (9%) with transverse ridges (8%) or longitudinal ridges (5%) and anomalous, completely flat bulbs (9%) (these latter possibly due to the bipolar technique) are also present.

Mistakes or difficulties during the production sequence are testified to by the irregular ventral surface of the flakes, often due to cleavage planes, by overshoot (5 items) or hinge (six items) terminations and by five Siret fractures.

## Retouched Blanks (Fig. 7; SI Fig. S3)

The retouched blanks are 19% (30 items) of the total assemblage suitable for use (161 items) (Table 4). According to Bordes classification (Bordes & Vaufray, 1961), almost half of the retouched flakes consists of side scrapers (straight, convex, or concave-convex), convergent side scrapers (déjété or convex). Two atypical end-scrapers, one atypical piercer, two notch-denticulate, one small chopper, and seven retouched flakes are also present. The retouch is direct, scalar, or rarely sub-parallel.

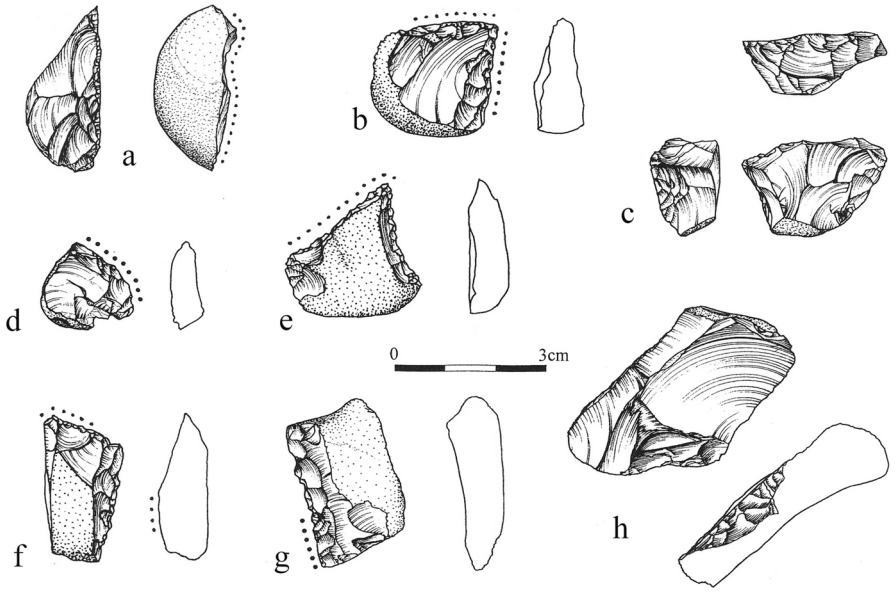


**Fig. 7** Retouched tools. Lateral scrapers (a, d, g, h); convergent scrapers (b, c, e, f). Dots document use-wear

**Table 4** Typological classification of the retouched lithic items

| Retouched Items | | | |
|---|---|---|---|
| Type | Quantity | RMU | Use-wear |
| Chopper | 1 | 1 | 1 |
| Side-scrapers (straight or convex) | 8 | – | 4 |
| Convergent side-scrapers (convex or déjetés) | 5 | – | 4 |
| Notches and denticulated | 2 | 1 | 1 |
| Piercer | 1 | 1 | – |
| Atipical end-scrapers | 2 | – | – |
| Retouched cores | 3 | – | 2 |
| Retouched flakes | 6 | 1 | 2 |
| Fragments of retouched tool | 2 | – | 1 |
| Total | 30 | 4 | 15 |

A modification by resharpening was observed on the retouched edges of two scrapers and on the chopper.

The retouched blanks consist mostly of flakes. The retouched cores are four in total; except for the small chopper, the limited retouched portions of the remaining three cores do not allow for a typological definition of these items. Only the half of the retouched items was actually used, with a prevailing activity of scraping (ratio 2:1); on the contrary, the flakes were mostly used to cut.

## Refitting

Twenty-eight raw material units (hereafter indicated as RMUs) were identified (Figs. 8, 9; SIFigs. 4–46). These RMUs consist of a minimum of two and maximum of fourteen items for a total of 111 artifacts. Eighty-nine refitted blanks were positioned on the excavation grid; the remaining 22 blanks were found during the sieving procedure; thus, for the latter, the location was limited to the square/spit of the deposit sieved. Every single piece of the lithic assemblage was included in the refitting analysis (for the analytical description of the refitting see the SI). The items involved in the RMU constitute 18% of the whole lithic assemblage; the blanks suitable for use, however, compose 49% of the whole usable lithic assemblage.

Many RMUs document just a part of the total configuration even if, in a few cases, they are almost complete (Table 5). Moreover, there are fragments of the same blank that refit (Table 5) and blanks that relate to an RMU for their general characteristics even if they do not refit.

In 13 RMUs, cores were missing. These RMUs are made up of two or, more rarely, three items that conjoin or that were assumed to pertain to the same RMU for their general characteristics (raw material, blank morphology, and dimensions). They document biased production sequences related to the initial steps (external cortical flakes) or to the advanced steps (internal flakes) of the reduction.

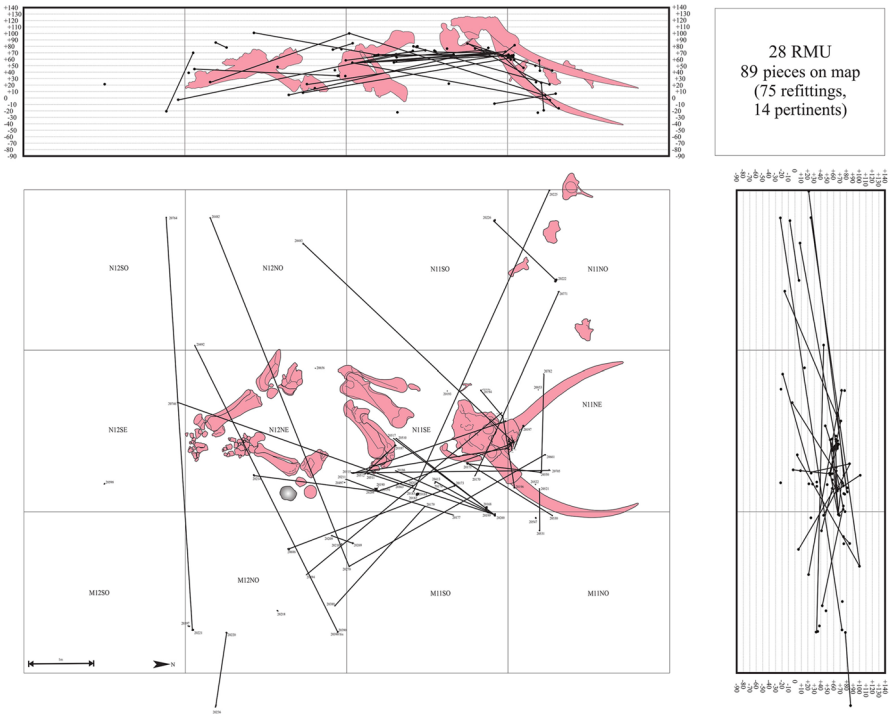


**Fig. 8** Plan and sections with the positioned pieces of the 28 identified RMUs and refitting lines

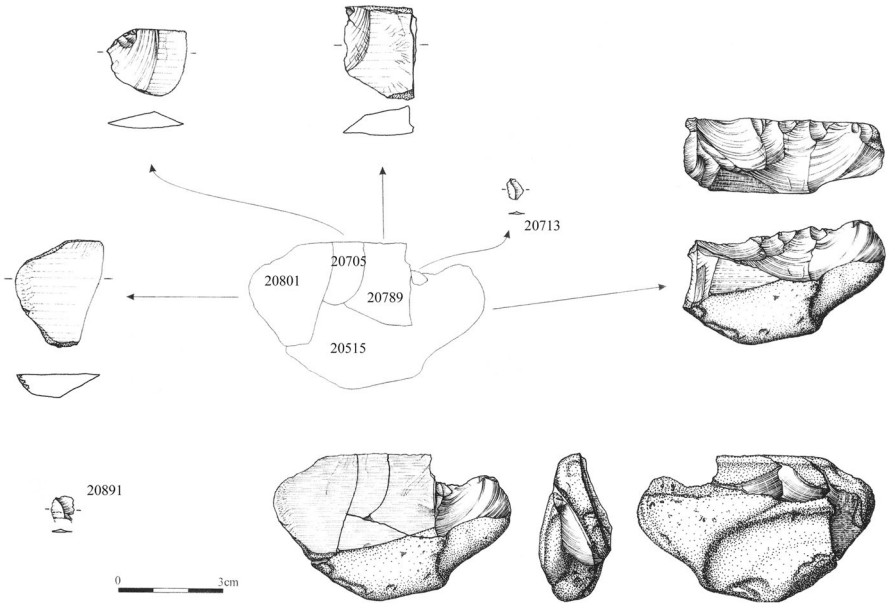


**Fig. 9** RMU 14 (drawing)

The remaining 15 RMUs comprise the refitting with the cores present. The RMUs on cores on pebble are the most complete in terms of volume and number of items that refit. In one case, in addition to the primary core, the RMU was composed of a core-on-flake pertaining to the initial steps of the reduction.

On average, the missing blanks were approximately half of the entire production testified to by the RMUs. The estimation, when possible, of the technological and morphological characteristics of the missing blanks did not highlight recurrences on dimensions and steps of the production sequence (Table 6).

It is worth mentioning that few retouched tools are associated with RMUs. They number 1 conjoining and 4 refitting; two of them comprise cores, documenting the production and the shaping of the retouched tools on the spot. Three out of four showed use-wear (1 conjoining and 2 refitting). Only 4 used flakes pertain to the RMUs; three of them are part of refitting that comprise cores, documenting the production of these items on the spot.

## Residues Analysis

Residue analysis was applied to the 29 lithic items showing a good state of preservation and active edges with traces of use (edge-removals and edge-rounding) detected by a stereomicroscope with a reflected light system (see also the "Multivariate Analysis of the Infrared Data" section). The residue analysis applied to a control sample of three lithic items without traces of use (ID 20803, ID 2390, ID 2886) did not provide any result.

**Table 5** Details of the identified RMU

| RMU | N° | Refitted | Conjoined | Pertinent | On map | Sieve | Use-Wear | Total |
|---|---|---|---|---|---|---|---|---|
| With refitted | 1 | 2 | - | - | 2 | - | | 2 |
| | 2 | 7 | 2 | 1 | 8 | 2 | | 10 |
| | 3 | 2 | - | 1 | 3 | - | | 3 |
| | 4 | 3 | 2 | - | 5 | - | 20191+20214 | 5 |
| | 5 | 9 | 2 | 3 | 12 | 2 | | 14 |
| | 6 | 2 | - | - | 2 | - | | 2 |
| | 7 | 2 | 2 | 1 | 5 | - | 20550 | 5 |
| | 8 | 2 | 1 | - | 3 | - | | 3 |
| | 10 | 2 | - | - | 2 | - | | 2 |
| | 12 | 2 | - | 1 | 1 | 2 | | 3 |
| | 13 | 2 | - | - | 2 | - | | 2 |
| | 14 | 5 | - | 1 | 5 | 1 | | 6 |
| | 15 | 2 | - | - | 2 | - | | 2 |
| | 17 | 2 | 1 | - | 3 | - | 20390 bis | 3 |
| | 18 | 7 | 1 | 1 | 8 | 1 | | 9 |
| | 19 | 2 | - | - | 2 | - | 20805 | 2 |
| | 20 | 7 | - | 2 | 8 | 1 | | 9 |
| | 22 | 2 | - | - | 2 | - | | 2 |
| | 25 | 2 | - | 1 | 3 | - | 20221 | 3 |
| | 26 | 3 | - | 2 | 3 | 2 | | 5 |
| | 28 | 2 | - | - | 2 | - | | 2 |
| | Total | 69 | 11 | 14 | 83 | 11 | | 94 |
| Only Conjoined | 9 | - | 2 | - | 2 | - | | 2 |
| | 16 | - | 2 | - | 2 | - | | 2 |
| | 30 | - | 2 | - | - | 2 | | 2 |
| | Total | - | 6 | - | 4 | 2 | | 6 |
| Only pertinent | 11 | - | - | 2 | 1 | 1 | | 2 |
| | 21 | - | - | 2 | 1 | 1 | 20598 | 2 |
| | 23 | - | - | 2 | - | 2 | | 2 |
| | 27 | - | - | 3 | - | 3 | | 3 |
| | 31 | - | - | 2 | 2 | - | | 2 |
| | Total | - | - | 11 | 4 | 7 | | 11 |
| Total | | 69 | 17 | 25 | 91 | 20 | | 111 |

## Morphological Analysis, SEM–EDX Analysis

The observation sample at low magnification using the RH-Hirox did not yield significant results. The application of the stain technique on micro-residues was more successful. The biochemical stain allowed highlighting the remains of collagen (Table 7; Fig. 10), which appeared with a specific color when the sample was observed in crossed polarized light, distinguishing them from the color and birefringence that characterize plant tissues. Picro-Sirius Red was tested on experimental animal tissue samples (i.e., skeletal muscle, bone, cartilage, hide, and tendons), producing a large reference collection (Caricola *et al.*, 2022). The collagen reacts to the biochemical stain and appears in cross-polarized light showing a red, green, and yellow-orange coloring.

The archaeological samples analyzed returned some amorphous portions of collagen (size range approximately 40 μm) that reacted to the Picro-Sirius Red with a

**Table 6** Raw material units that include cores

| RMU | Core/s | Flakes | Flake's fragments | Processing waste | Volumetric completeness % | Total of usable products[1] | Usable missing products |
|---|---|---|---|---|---|---|---|
| 1 | 1 | 1 | – | – | 100% | 1 | – |
| 2 | 1 | 5 | 1 | 1 | 75–100% | 7(E) | 2(E) |
| 3 | 1 | 1 | 1 | – | 50–75% (E) | ≥8(E) | ≥6(E) |
| 4 | 1 | 1 | 2 | 1 | 75–100% | 4(E) | 2(E) |
| 5 | 2 | 7 | – | 5 | ? | ≥10(E) | ≥2(E) |
| 6 | 1 | 1 | – | | ? | ? | ? |
| 7 | 1 | 2 | – | 2 | 50–75% (E) | ≥8(E) | ≥6(E) |
| 8 | 1 | – | 2 | – | 50–75% (E) | ≥3(E) | ≥2(E) |
| 14 | 1 | 3 | – | 2 | 75–100% | 5 | 2 |
| 15 | 1 | 1 | – | – | 25–50% | ≥2(E) | ≥1(E) |
| 18 | 1 | 5 | – | 3 | 75–100% | ≥7(E) | ≥4(E) |
| 19 | 1 | 1 | – | – | ? | ≥4(E) | ≥3(E) |
| 20 | 1 | 3 | – | 5 | 75–100% | ≥5(E) | ≥3(E) |
| 25 | 1 | 2 | – | – | 50–75% (E) | ≥4(E) | ≥2(E) |
| 26 | 1 | 2 | – | 2 | 25–50% (E) | ≥5(E) | ≥3(E) |
| 28 | 1 | 1 | – | – | 25–50% (E) | ≥4(E) | ≥3(E) |

[1]Excluding cores

*(E)* estimated

yellow color in transmitted light and green-yellow in cross-polarized light with a low birefringence. It is not possible to attribute this amorphous residue to a specific tissue. In the sample, no other residues were identified. Some vegetable fibers could be interpreted as contamination, which also occurred in ancient times. Additionally, some samples that reacted to the biochemical stain (PSR) returned FTIR bands compatible with proteinaceous materials and adipocere (i.e., samples 20126; 20390bis).

The observation at SEM detected, in the area of the active edge of four items (ID 20216, ID 20514, ID 20635, ID 20653), the presence of few oriented spots of micro-residues (Fig. 11a); EDS analysis of the micro-residues documented a Ca/P atomic ratio equal to ~ 2.1 (Fig. 11b; Table 7) characteristic of the mineral component of the bone, the hydroxyapatite (Ellingham *et al*., 2017; see also Hayes & Rots, 2019; Perdegnana & Ollé, 2018; Venditti *et al*., 2021a, b).

## FTIR

Microresidues were observed in 27 lithic items (Table 7), with a focus on different areas of the artifact (active edges, internal surfaces), thus obtaining an infrared dataset comprising 92 spectra.

The spectral features detected in the range 400–4000 $cm^{-1}$ could be divided into two categories: the intense Reststrahlen bands detected in the 400–1300 $cm^{-1}$ region due to the specular reflectivity of the flint and the weak absorption bands observed

**Table 7** Results of the residues and use-wear analyses

| Sample | Type | Vibrations frequency ($cm^{-1}$) | SEM–EDX | STAIN (PSR) | Use-wear (material worked) | Use-wear (action carried out) |
|---|---|---|---|---|---|---|
| 20126 | Retouched flake | 2916 w, 2847 w, 1655 w br, 1575 w, 1538 w, 1465 vw br | | Amorphous collagen | Meat + Fresh hide | Cutting |
| 20169 | Core fragment | 2915 w, 2848 w, 1655 w br, 1575 w, 1538 w, 1645 w br, ~913 sh | | | Soft material | Scraping |
| 20185 | Flake | 2916 w, 2847 w, 1575 w, 1538 w, 1465 vw br | | | Meat | Indeterminable |
| 20191 | Core | 2915 w, 2847 w, 1653 w br, 1575 w, 1538 w, 1463 vw br | | | Soft material | Scraping |
| 20214 | Flake | 2914 w, 2847 w, 1653 w br, 1573 w, 1539 w, 1463 vw br, ~913 sh | | | Hide | Scraping |
| 20216 | Retouched flake | 2914 vw, 2847 vw, | 1 C, O, F, Si, P + Ca | | Meat + Fresh hide | Scraping |
| 20217 | Flake | 1653 vw br, | | | Soft material | Cutting |
| 20221 | Chopper | ~913 sh | | Amorphous collagen | Bone | Scraping |
| 20234 | Retouched flake fragment | 2917 w, 2847 w, 1653 w br, 1576 w, 1540 w, 1460 vw br | | | Meat | Cutting |
| 20235 | Flake | 2916 w, 2847 w, 1653 w br, 1577 w, 1540 w, 1460 vw br | | Amorphous collagen | Meat + fresh hide | Indeterminable |
| 20271 | Retouched flake | 2914 w, 2849 w, 1650 w br, 1540 w br, 1460 vw br 1648 w br, 1540 w br | | | Wood over hide | Scraping |
| 20463 | Flake | 2914 w, 2847 w, 1650 w br, 1574 w, 1538w, 1460 vw br | | | Soft material | Scraping |
| 20484 | Retouched flake | | | | Soft material | Scraping |

**Table 7** (continued)

| Sample | Type | Vibrations frequency ($cm^{-1}$) | SEM–EDX | STAIN (PSR) | Use-wear (material worked) | Use-wear (action carried out) |
|---|---|---|---|---|---|---|
| 2039bis | Retouched flake fragment | 2914 w, 2847 w, 1650 w br, 1574 w, 1538w, ~913 sh | | Amorphous collagen | Soft material | Cutting |
| 20514 | Retouched flake | | 1 C, O, Si, P + Ca | Amorphous collagen | Fresh hide | Cutting + Scraping |
| 20516 | Flake | 2914 w, 2847 w, 1650 w br, 1574 w, 1538w, 1460 vw br | | | Meat | Cutting |
| 20537 | Flake | 2914 w, 2847 w, 1650 w br, 1574 w, 1538w, 1460 vw br | | | Soft material | Cutting |
| 20546 | Retouched flake fragment | 2914 w, 2847 w, 1650 w br, 1574 w, 1538w, ~913 sh | | | Soft material | Scraping |
| 20550 | Flake | 2914 w, 2847 w, 1650 w br, 1574 w, 1538w | | | Soft material | Cutting + Scraping |
| 20598 | Retouched flake | 2914 w, 2847 w, 1650 w br, 1574 w, 1538w, 1460 vw br | | | Meat | Indeterminable |
| 20635 | Flake | 2914 w, 2847 w, 1650 w br, 1574 w, 1538w, 1460 vw br | 1 C, O, Si, P + Ca, S | | Indeterminabile | Wedging |
| 20653 | Retouched flake | 2914 w, 2847 w, 1650 w br, 1574 w, 1538w, 1460 vw br | 1 C, O, D, Si, P + Ca | | Meat + bone | Cutting |
| 20679 | MFL fragment | 2914 w, 2847 w, 1650 w br, 1574 w, 1538w, ~913 sh | | | Soft material | Cutting |

**Table 7** (continued)

| Sample | Type | Vibrations frequency ($cm^{-1}$) | SEM–EDX | STAIN (PSR) | Use-wear (material worked) | Use-wear (action carried out) |
|---|---|---|---|---|---|---|
| 20785 | Retouched flake fragment | 2914 w, 2847 w, 1650 w br, 1574 w, 1538w, 1460 vw br | | | Meat + fresh hide | Cutting + Scraping |
| 20796 | Retouched core on flake | | | | Meat | Cutting |
| 20805 | Flake | 2914 w, 2847 w, 1650 w br, 1574 w, 1538w | | | Wood | Cutting |
| 20825 | Retouched flake | 2914 w, 2847 w, 1574 w, 1538w | | | Fresh hide | Scraping |
| 20832 | Flake | 2914 w, 2847 w, 1574 w, 1538w | | | Meat + other indeterminable material | Scraping |
| 21020 | MFL retouched | 2914 w, 2847 w, 1574 w, 1538w | | | Meat | Indeterminable |

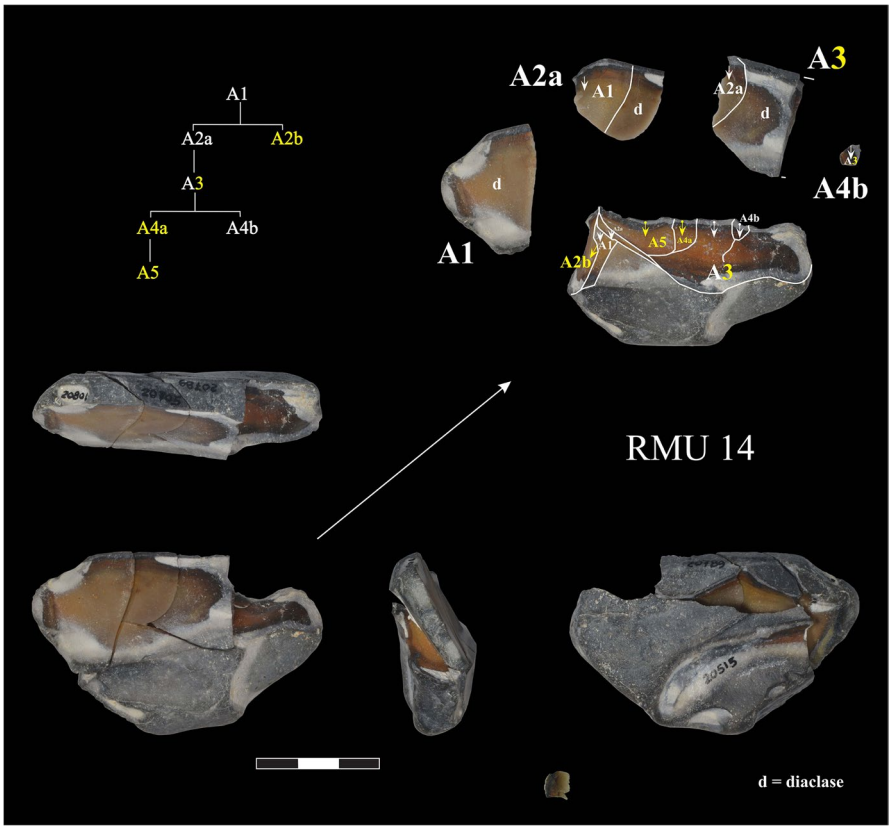


**Fig. 10** RMU 14 (photo and diacritical scheme)

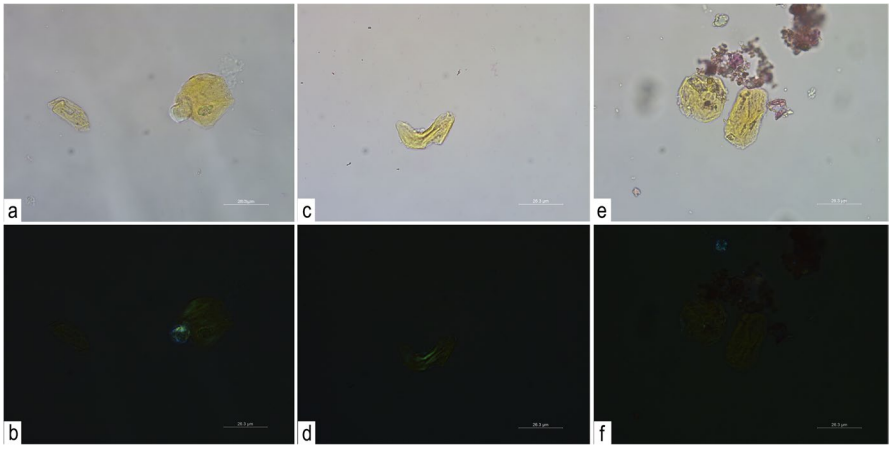


**Fig. 11** Amorphous portions of collagen found on Polledrara stone tools. The residues appear yellow in color in transmitted light (**a**, **c**, **e**) and green in cross-polarized light with low-medium birefringence (**b**, **d**, **f**)

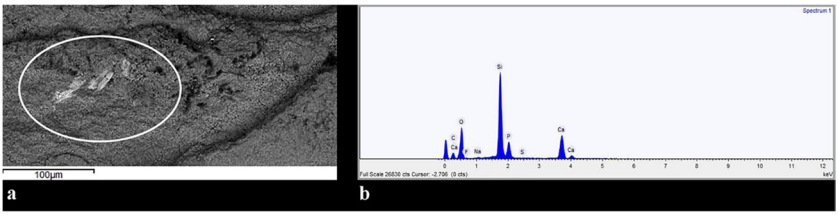


**Fig. 12** SEM–EDX residues analysis. Bone residues (**a**) and their elemental fingerprint, Ca/P atomic ratio equal to ~ 2.1 (**b**)

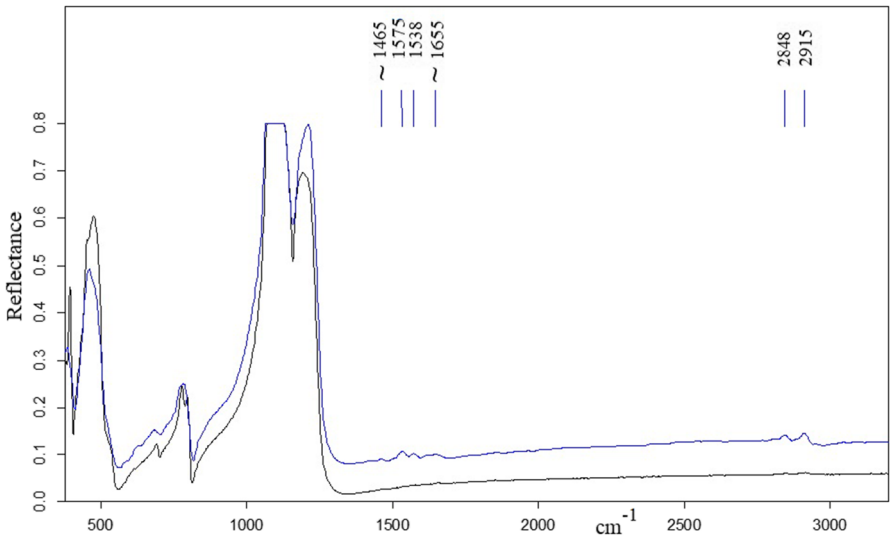


**Fig. 13** Micro-FTIR spectra of lithic tool 20169 of unused portion of the tool (black) and ventral edge (blue) showing proteinic residues

wwwbetween 1400 and 1850 $cm^{-1}$ and in the range 2700–3050 $cm^{-1}$. These latter are considered fingerprints of the embedded molecular species, since absorption features approximately 1600 $cm^{-1}$ are typically due to amides and those between 2700 and 3050 $cm^{-1}$ are due to the CH stretching vibrational modes. An example of an extended spectrum is reported in Fig. 12, where the molecular absorption bands are highlighted in the insets. Occasionally, a band centered at 913 $cm^{-1}$ (Fig. 13) was detected in the reflectance, probably assignable to hydroxyapatites or kaolin (aluminum silicate) residues (Tironia *et al*., 2012). The Reststrahlen bands do not provide information on the usage of lithic tools, whereas the low intensity molecular fingerprints can be associated with organic residues entrapped on the micropores of the surface of the tools during their use; therefore, our analysis considers only these spectral features (Fig. 14). Spectra of the chemical fingerprints were baselined and normalized with standard procedures (Nucara *et al*., 2020) and the average spectra, *S**, was then calculated (Fig. 15) in both amide and CH stretching regions. In the

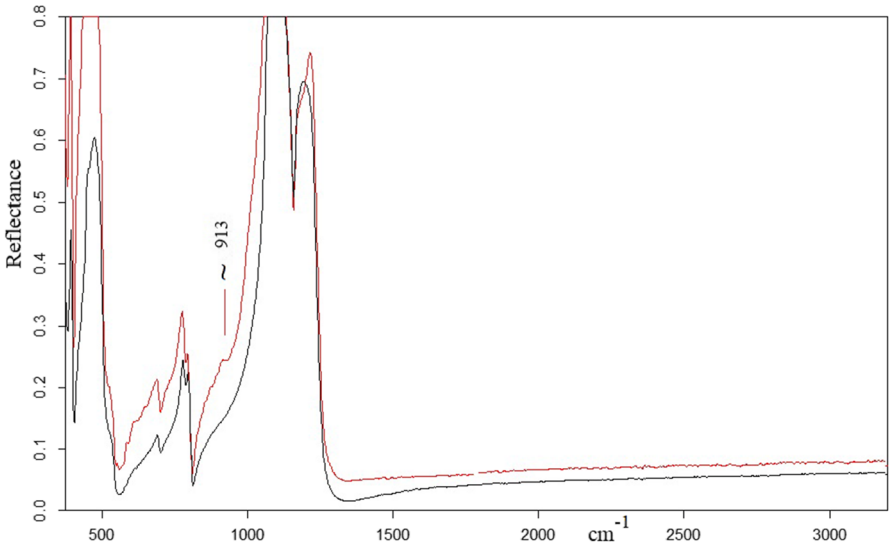


**Fig. 14** Micro-FTIR spectra of lithic tool 20169 of unused portion of the tool (black) and ventral edge (red) showing inorganic residues

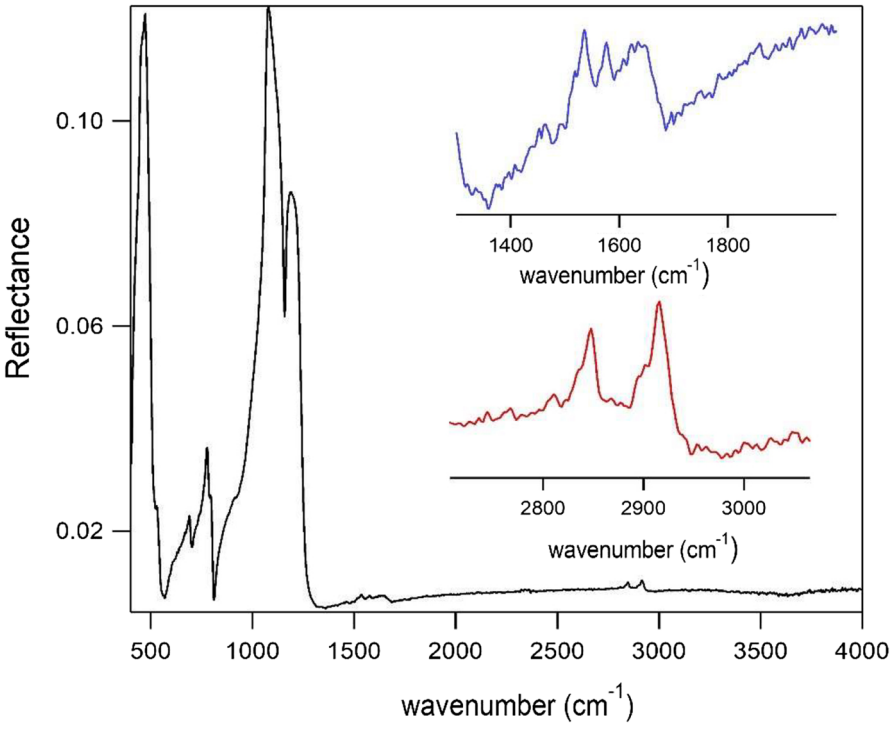


**Fig. 15** Raw reflectance spectrum of a selected sample. The intense Reststrahlen bands at 469769, and 1157 $cm^{-1}$ are due to SiO vibration of flint. The regions of the vibrational fingerprints from organic residues are reported in enlarged scale in the insets

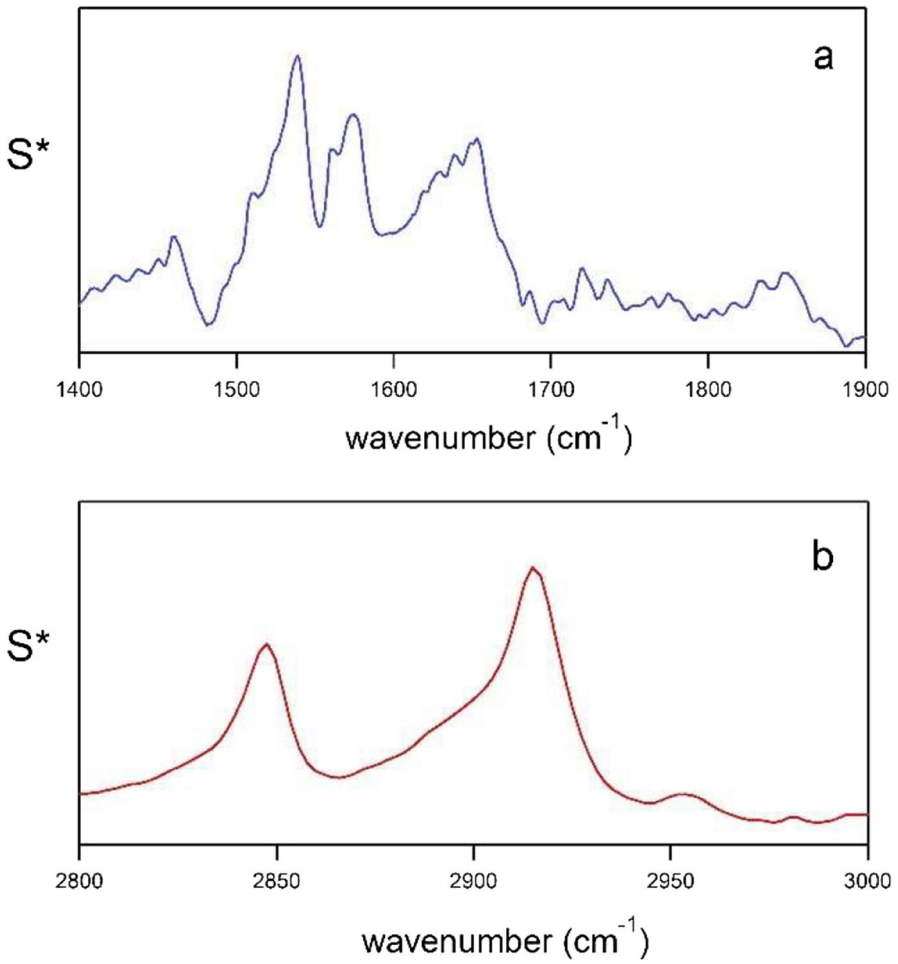


**Fig. 16** The average spectra *S** in the fingerprint region of amides (**a**) and in the CH stretching region (**b**)

*S** spectra, the absorption lines appeared broadened by the overlapping of several contributions and by the spatial inhomogeneity of the samples, but a likely assignment of the vibrational mode was feasible based on previous results in the literature (Gremlich & Bing, 2001). In the amide region (Fig. 15a, b), we resolved a line approximately 1450 $cm^{-1}$ that was putatively assigned either to C–H bending modes or to $CaCO_3$: the former assignment provides a trace marker for lipids and fats. In the same spectral region, the doublet of lines at 1539 and 1574 $cm^{-1}$ attested to the presence of fat in the form of adipocere, often observed in ancient stone tools (Forbes *et al*., 2004). However, the most relevant feature in this region was the band centered at 1650 $cm^{-1}$, assignable to amide absorption of proteinaceous materials. Notably, the amide II band (N–H bending was not resolved in the spectrum, as it was hidden by the most intense adipocere contributions. Less intense bands were

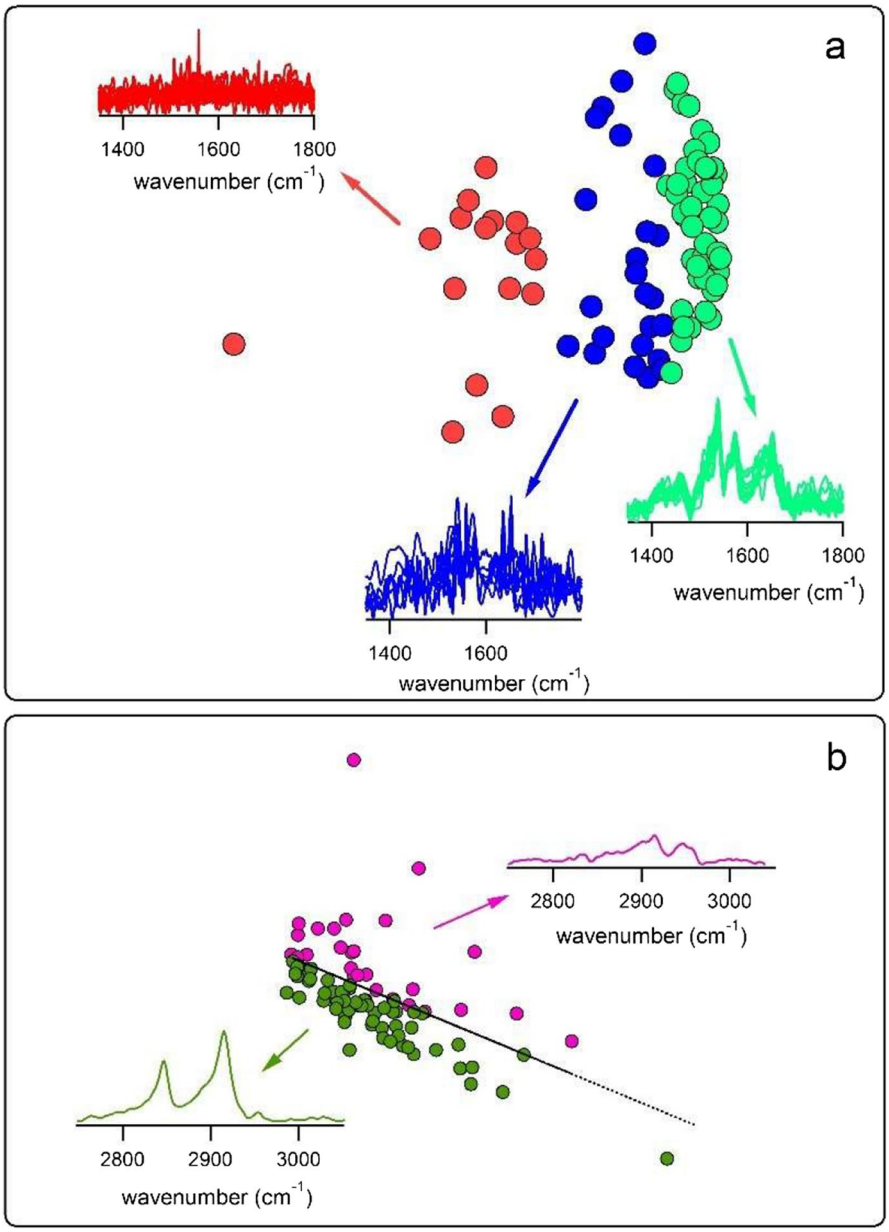


**Fig. 17** **a** the S1 (65% of the explained variance, horizontal axis) and S2 (4%, vertical) plane obtained from a PCA analysis of spectra in the amide region. The coordinate axes are omitted for sake of clarity. **b** The S1 (94% of the explained variance) and S2 (3%) plane from spectra in the CH stretching region

barely detected at approximately 1720 (C=O stretching of esters) and 1840 $cm^{-1}$. Regarding the average spectra in the CH stretching region shown in Fig. 15b , the symmetric and asymmetric $CH_2$ vibrational modes are well resolved at 2847 and

**Table 8** PCA analysis results

| Sample | No. residues | Y | U | N | P/100 |
|---|---|---|---|---|---|
| 20214 | 3 | • | •• | | 0.47 ÷ 0.67 |
| 20390bis | 5 | ••• | | •• | 0.60 |
| 20126 | 2 | •• | | | 1.0 |
| 20169 | 2 | • | | • | 0.50 |
| 20185 | 2 | •• | | | 1.0 |
| 20191 | 3 | ••• | | | 1.0 |
| 20216 | 4 | •• | | •• | 0.50 |
| 20217 | 2 | • | • | | 0.6 ÷ 0.75 |
| 20221 | 4 | • | • | •• | 0.3 ÷ 0.37 |
| 20234 | 5 | ••• | •• | | 0.68 ÷ 0.8 |
| 20235 | 2 | • | • | | 0.6 ÷ 0.75 |
| 20271 | 4 | •••• | | | 1.0 |
| 20463 | 2 | | • | • | 0.1 ÷ 0.25 |
| 20516 | 7 | ••••• | | •• | 0.71 |
| 20537 | 2 | •• | | | 1.0 |
| 20546 | 2 | • | | • | 0.5 |
| 20550 | 2 | | • | • | 0.1 ÷ 0.25 |
| 20,598 | 2 | | | •• | 0.0 |
| 20635 | 4 | •••• | | | 1.0 |
| 20653 | 5 | •• | •• | • | 0.48 ÷ 0.6 |
| 20679 | 3 | ••• | | | 1.0 |
| 20785 | 3 | • | • | • | 0.4 ÷ 0.50 |
| 20805 | 1 | • | | | 1.0 |
| 20825 | 4 | •••• | | | 1.0 |
| 20832 | 4 | ••• | | • | 0.75 |
| 21020 | 2 | •• | | | 1.0 |

2916 $cm^{-1}$, respectively. The weak band at 2960 $cm^{-1}$ suggests $CH_3$ stretching vibration. The simultaneous occurrence of both fat and protein features in the spectra supports the assumption that archaeological artifacts were used on organic materials of animal origin. However, a refined distinction between the different tools can be attained by a multivariate analysis of the spectra: indeed, under the reasonable hypothesis that the lithic tools used for organic material processing would be rich in protein and fat residues, PCA provides a feasible approach for artifact recognition and classification.

## Multivariate Analysis of the Infrared Data

PCA of the 92 infrared spectra (from different samples and sample areas) was performed according to the procedure reported in Caporaletti *et al*. (2017). The matrix of the absorption intensities (matrix dimension N × M, with $N$ = number of spectra

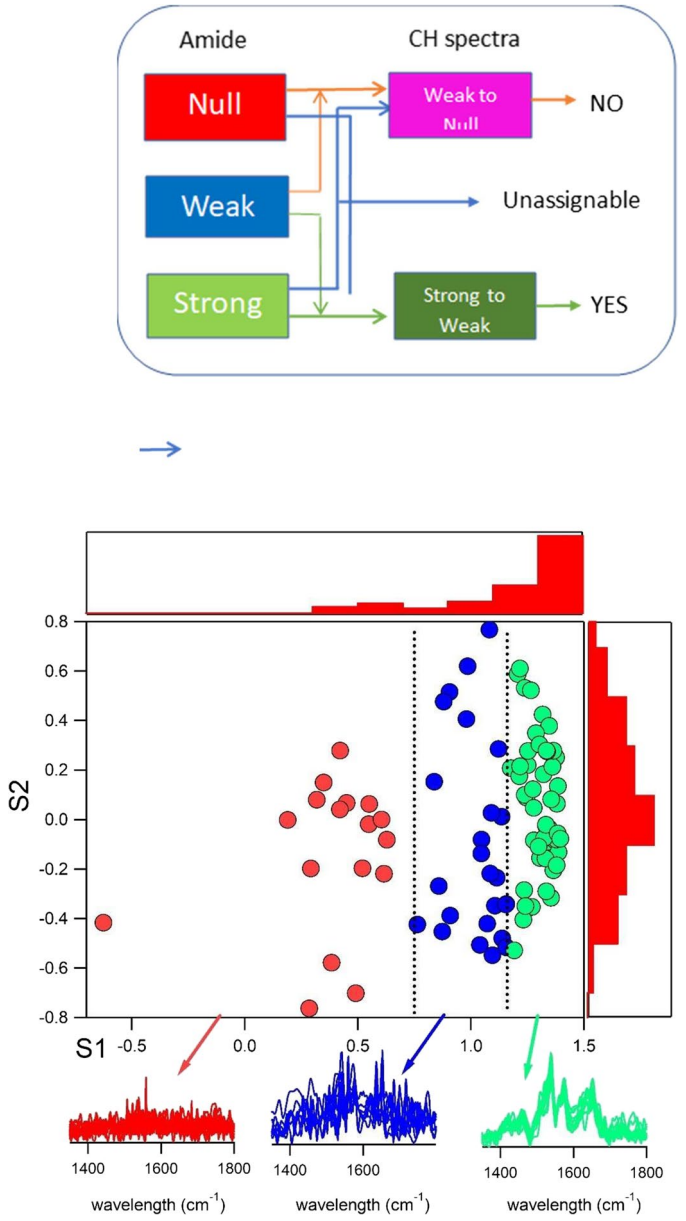


**Fig. 18** Problem to solve: "Does the trace contain organic materials?" According to the PCA analysis of the infrared data, there are three pathways to answer the question: green lines yield a favorable answer, the red ones to reject the hypothesis. The blue lines drive toward unclear answer

and $M =$ number of data points) was processed with commercial and in-house codes, all based on NIPALS algorithms (Wright, 2017). The analysis was carried out in different sessions for the two fingerprint regions (amides and CH stretching regions)

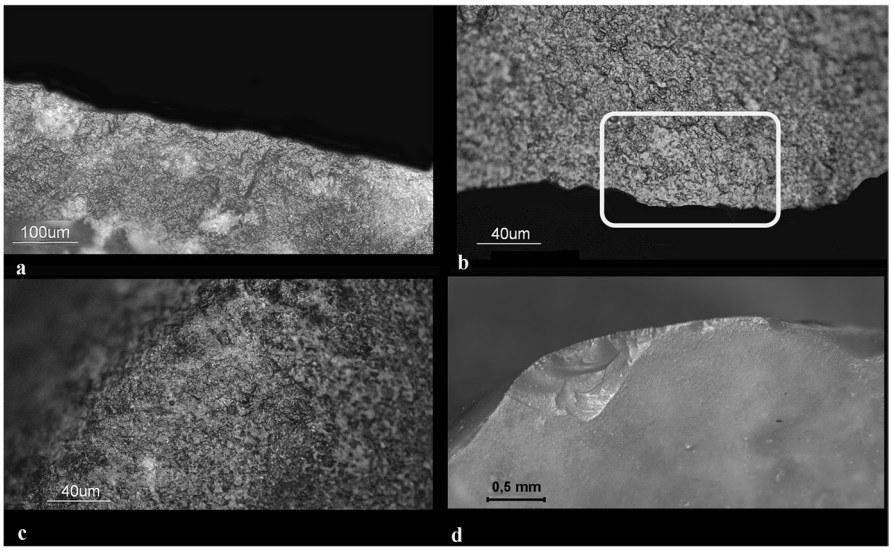


**Fig. 19** Residual use-wear and griping traces observed on the lithic tools. ID 21020, thin line of rough to smooth polish and edge-rounding related to soft animal tissues on the butt of a micro-flake (**a**); ID 20825, residual smooth domed to flat polish related to hide on a resharpened active edge (**b**); ID 20825, large spot of rough, flat polish with striae (**c**) and ID 20832, localized small close-regular edge removals overlapping large edge removals opposite to the active edge, related to gripping

and the findings of each session were finally cross-linked to determine the most likely use of the artifacts. For both spectral regions, scores 1 (S1) and 2 (S2) represented the most meaningful PCA outcomes, since S1 (S2) provided the first (second) order statistical displacements from $S^*$ of each spectrum (Todeschini, 1998). Panel a of Fig. 16 shows S1-S2 plane, as obtained from the multivariate analysis in the amide region.

In this panel, three clusters of data can be distinguished, according to the different values of S1; the one in light green points tags spectra with well-resolved absorption lines in the amide region and spectral shape close to the average spectrum $S^*$, while spectra with moderate intensity of the amide features (blue dots) and/or noisy spectra (red) are represented by the other clusters. The PCA of spectra in the CH region provides similar results, but points on the S1-S2 plane are less detached than the previous case (panel b in Fig. 16). Points in the S1-S2 plane reported in panel b are approximately aligned along a line that separates the plane itself into two halves. Dark green points below this line identify spectra with intense CH absorption bands, while magenta data are placed on the upper side of the plane tag spectra with the weakest intensity. The magenta outlier data represent spectra with vanishingly small CH intensities.

The question of whether the archaeological artifacts were used on organic materials can be addressed in two steps. First, by cross-referencing the PCA results in both spectral regions, spectra of the traces can be grouped in different classes: the rationale is summarized in the cartoon in Fig. 17; spectra showing the simultaneous

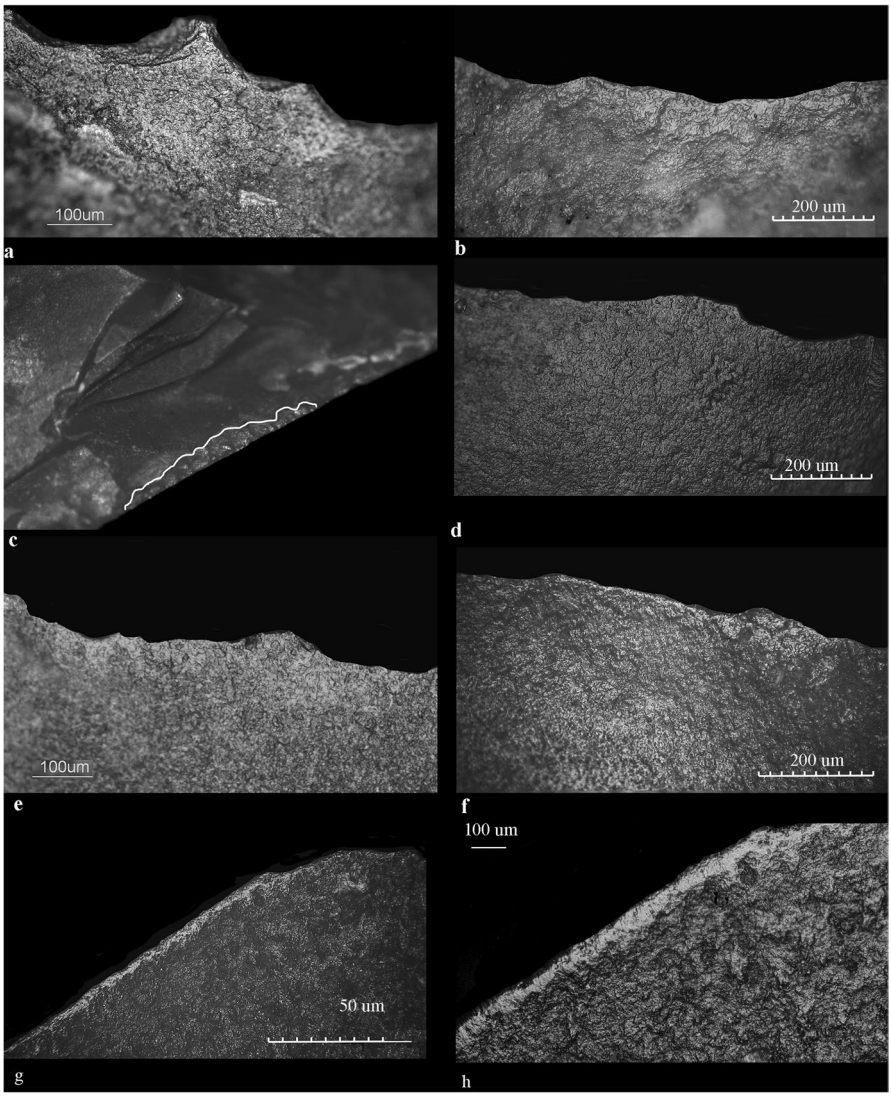


**Fig. 20** Use-wear observed on the lithic tools. Band of rough to smooth polish with granular topography related to meat working (ID 20516 **a**, ID 20598 **b**, ID 20796 **d**, ID 20832 **e**); ID 20796, close-regular, feather termination edge removals related to soft material working (**c**); outer edge line of smooth polish combined with edge-rounding related to the contact with hide (ID 20514 **f**, ID 20214 g–**h**)

presence of intense amide bands and CH contributions (green pathway to YES in the figure) are associated with the highest probability that the corresponding lithic tool worked meat and fat. The same occurrence must be rejected for spectra of residues with null or negligibly small absorption in both spectral regions (red line to NO). Similar assessments are challenging for spectra with bands of absolutely different intensities in the two regions.

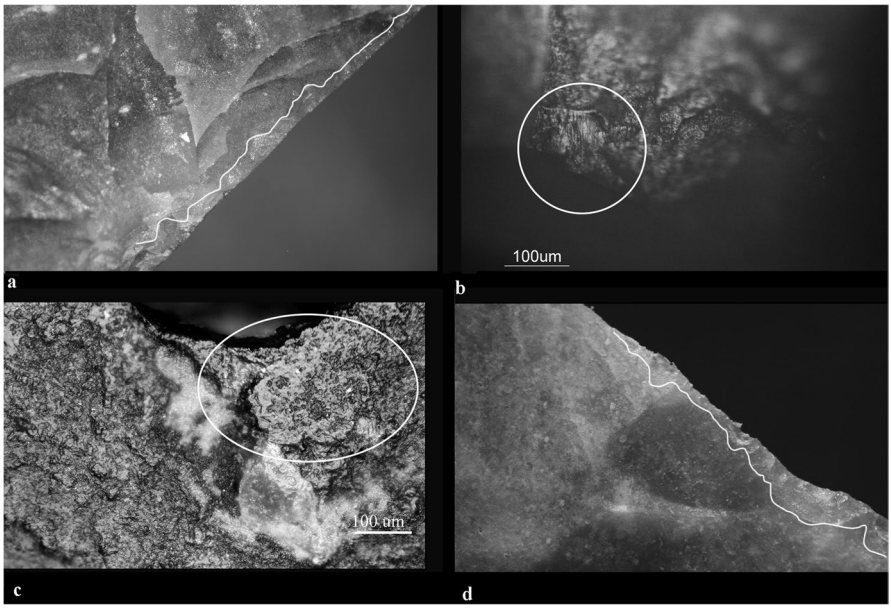


**Fig. 21** Use-wear on lithic tools. ID 20169, close-regular, feather-step edge-removals related to soft material working (**a**); ID 20221, spot of smooth flat polish with comet tails related to bone working (**b**); ID 20271, smooth, domed, reticulated polish related to wood working (**c**); ID 20550, close-regular, step-hinge edge removals related to medium hard material working (**d**)

A safe approach suggests assigning spectra with moderate intensity amide absorption (blue cluster in Fig. 17) either to the "YES" or the "NO" groups according to the results of PCA in the CH region (thin lines in Fig. 17). Notably, the spectra in the blue cluster equally contribute to the magenta and dark green ones. On the other hand, all those cases where intense and nonintense bands coexist in the same spectrum (blue lines in Fig. 17) must be considered scarcely reliable for the assignment of organic residues. This analysis leads to a first conclusion that 55 out of 92 traces undoubtedly contain organic residues, while 22 traces show no statistical evidence of organic absorption within the capability of the PCA-infrared approach. Furthermore, fifteen spectra cannot be unambiguously used to assign the residue in the traces. Table 8 reports all samples studied in the infrared reflectance experiments, together with the number of traces and their assignments. The second step to estimate the probability that a specific archaeological artifact was used to process organic materials accounts for the number of its traces belonging to the "yes," "no," or "unassignable" groups. We define this probability as

$$P = \frac{n_Y P_Y + n_U P_U + n_N P_N}{n_Y + n_U + n_N} \tag{1}$$

where $n_i$ ($i$ = yes, unassignable, no) is the number of traces with residues for each class of the PCA results and $P_\mathrm{i}$ is the probability that residue shows organic

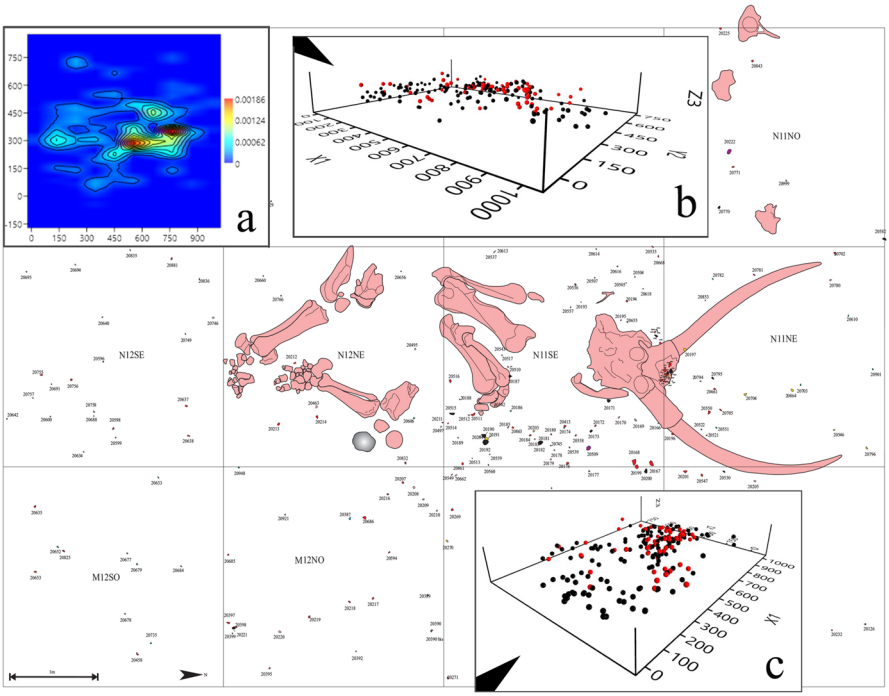


**Fig. 22** Distribution of lithic industry in the carcass area. On the background of the planimetry. (**a**) Kernel density estimation. (**b**, **c**) 3D graphics rendering (red dots represent the pieces belonging to the 28 RMUs)

fingerprints (thus, $P_Y = 1$ and $P_N = 0$). Concerning the fifteen unassignable spectra, we expected a conservative assumption for $P_U$, i.e., $0.2 < P_U < 0.5$. The probability $P$, according to Eq. 1, is reported in the sixth column of Table 8 for each sample: the uncertainty in $P_U$ provides the most reliable interval of values for $P$ in fifteen samples. However, even adopting conservative constraints on a priori *probability*, at least 21artifacts from the La Polledrara site were likely used in animal tissue processing.

## Use-Wear Analysis

The blanks ≥ 15 mm (161 items) found in the elephant area and represented by cores, flakes, and retouched flakes were analyzed at low and high magnification to detect the degree of preservation and the traces of use (see the "Methods" section). Sixty-two percent of the microflakes, microfragments, and indeterminable items (281 out of 455 items) were selected and analyzed. Microsurface modifications by use were found on 29 flakes: 27 from the former group of blanks ≥ 15 mm and 2 from the latter group of micro-items (Table 7).

The low percentage of artifacts with use-wear needs some words of clarification. Since the optimal preservation of the lithic surface of the artifacts (see

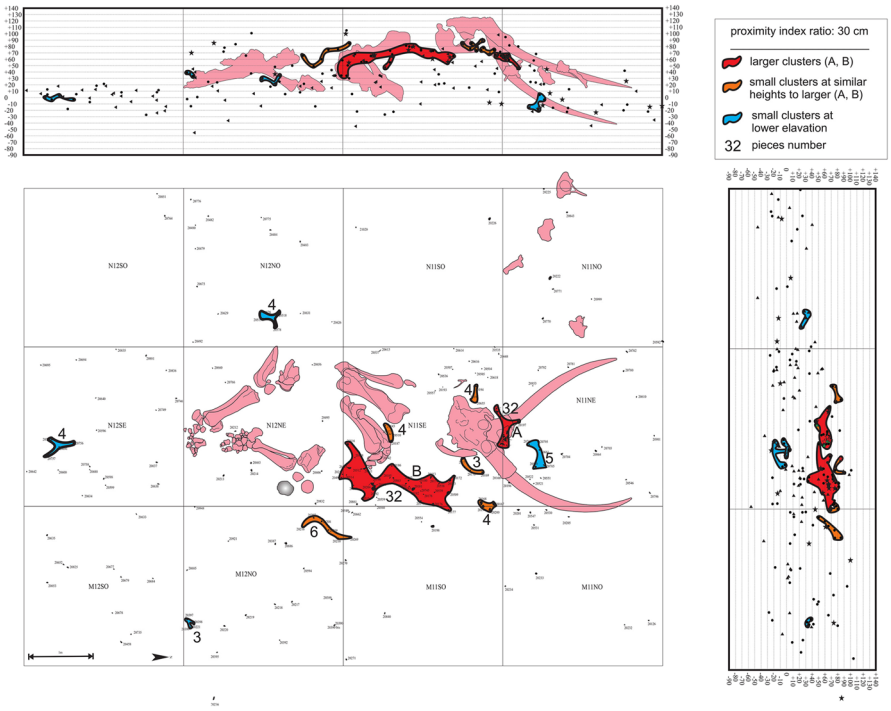


**Fig. 23** Clusters distribution resulting from the application of the proximity index

the "Cleaning Procedure" section), it is highly unlikely that the scarcity of the traces of use is the result of taphonomy processes. The low rate of the use-wear and the freshness of the surface suggest that a considerable part of the assemblage found in this area was unused. This evidence could indicate that few episodes of use were probably interspersed by knapping episodes (see the "Technological and Refitting Analyses" section) producing a substantial amount of debitage and debitage byproducts. In the "Use-Wear Analysis" section, these possible episodes are clarified and discussed on the basis of the data of the refitting analysis and the spatial analysis.

The artifacts with use-wear comprise 11 flakes, 8 retouched flakes, 4 retouched flake fragments, 1 chopper, 1 core, 1 core fragment, 1 indeterminate MFL fragment, 1 retouched core on flake, and 1 retouched MFL. The amount of the retouched artifacts (13 items $\geq$ 15 mm; 1 item $<$ 15 mm) is relevant in this assemblage, and it is quite equivalent to the amount of the debitage/cores with traces of use (14 items $\geq$ 15 mm; 1 item $<$ 15 mm). This evidence can be the result of the shaping and/or resharpening of the flakes knapped and used on the spot or the introduction of tools ready to be used, not related to the episodes of knapping that occurred at the site. The resharpening was confirmed by one microflake bearing traces of butchering (ID 21020) (Fig. 18a; see also Chan *et al.*, 2020 for a discussion of the use-wear observables on micro-debitage). Resharpening was suggested in two other cases: a retouched flake (ID 20825)

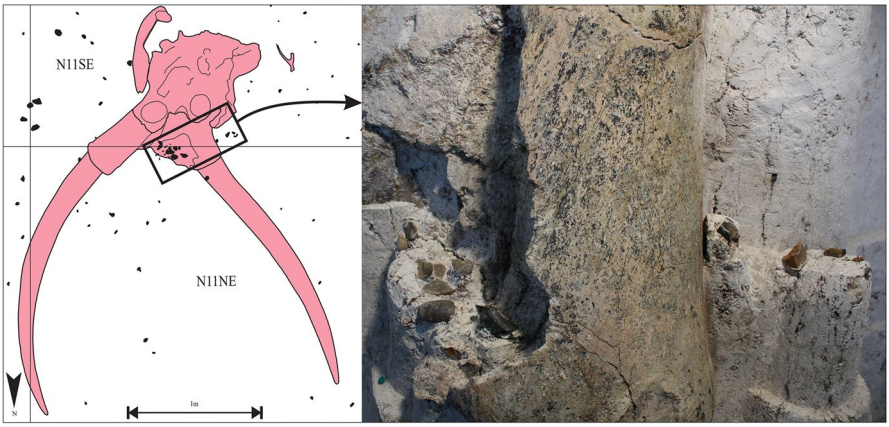


**Fig. 24** Cluster A. Localization on map and photographic detail

that showed remains of use-wear of hide processing quite entirely removed by retouching (Fig. 18b) and a retouched flake (ID 20216) that displayed lightly developed use-wear of hide/soft tissues; both lithic items displayed well-developed traces of prehension on the opposite side (Fig. 18c) (Zupancich *et al.*, 2016a). This discrepancy between the development of the traces of use and the trace of gripping suggests that this tool was used for a long time (traces of gripping) and its functional life ended shortly after its resharpening.

At La Polledrara, traces of hafting were not detected. Besides the two items showing well-developed polishes of prehension, seven more tools showed traces of prehension (ID 20214, 20271, 20484, 20537, 20598, 20653, 20832), consisting of very localized edge-removals opposite to the active (Fig. 18d) due to the punctual pressure exercised by the fingers on the tool (Rots, 2010).

Regarding the material worked, use-wear analysis documented that soft animal tissues were the major worked material (15 items, 52%) (Fig. 19a–h and SI Fig. S4 for reference collection comparison), followed by generic soft material (8 items, 28%). The generic soft material (Fig. 20a) was inferred through the analysis of the macrotraces only (ID 20169, 20191, 20217, 20390bis, 20463, 20484, 20537, 20679); the lack of microtraces on these items prevented the detailed interpretation of the material worked. Nevertheless, the relevant presence of lithic tools used to process soft animal tissues suggests that the generic soft material is very likely associated with the animal material.

The rare presence of harder material is testified to by the contact with bone (1 item, ID 20221) (Fig. 20b and SI Fig. 4 for reference collection comparison), wood (2 items ID 20271, ID 20805) (Fig. 20c), and generic medium hard material (2 items ID 20550, ID 20546) (Fig. 20d). It is worth also mentioning that in one case (ID 20271), traces of use on wood on the top of traces of soft animal material were detected.

Soft animal materials were processed with various actions (Table 7), cutting (4 items), scraping (3 items), and mixed (cutting + scraping) actions (2 items);

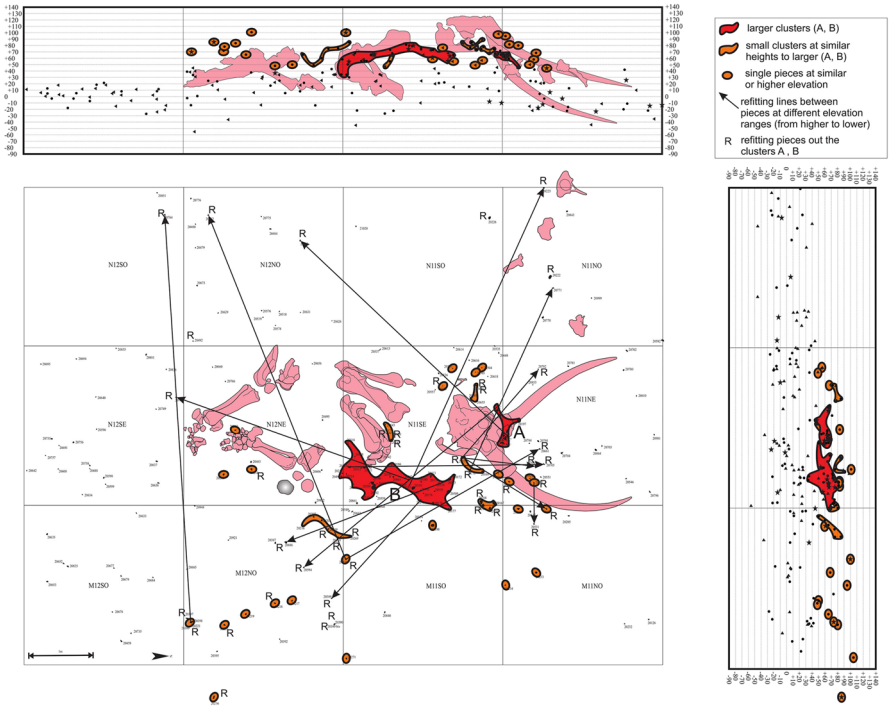


**Fig. 25** Clusters and single pieces at similar elevation are shown on the map refitting lines between pieces at different elevation range (arrows from higher to lower), and refitting pieces out the larger clusters

only the activities carried out with small fragments or microflakes were indeterminable due to the limited distribution of the use-wear. Any functional distinction between unretouched and retouched active edges was documented; cutting, scraping, and mixed actions were carried out independently with both categories of lithic tools.

Use-wear analysis allowed us to distinguish differences in the soft animal tissues. In fact, seven out of fifteen lithic tools (ID 20185, 20234, 20516, 20598, 20796, 20832, 21020) showed contact with meat only (Fig. 19a–b, d–e); one other lithic tool, in addition to meat, also showed contact with bone (ID 20221) and, finally, in the other seven cases (ID 20214, 20126, 20216, 20271, 2075, 20514, 20825), the lithic tools processed the inner surface of hide with cutting, scraping, or mixed action (Fig. 19f–h).

Only two items, one flake and one retouched flake, show the processing of a material other than animal tissues. These items worked wood, the flake by cutting (ID 20805), and the retouched flake by scraping (ID 20271). This latter item was previously used for processing soft animal material and reused for wood working without any reshaping of the active edge.

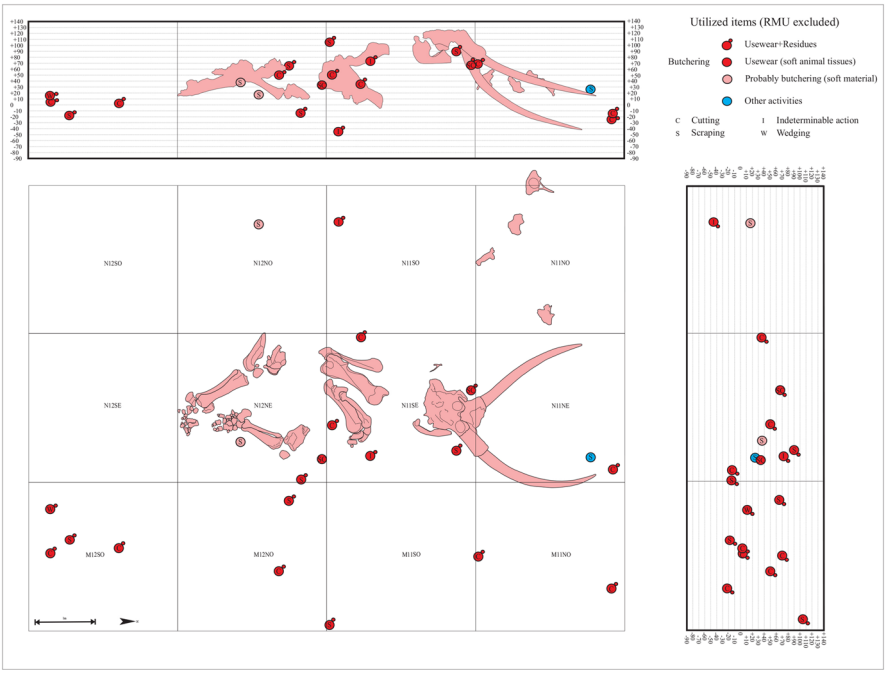


**Fig. 26** Spatial distribution of the used lithic tools not pertaining to RMUs

## Spatial Analysis

The spatial analysis was applied to the artifacts positioned in the excavation grid (Table 1). These artifacts represented 33% of the whole lithic assemblage found in the elephant area and 56% of all 29 RMUs identified (SI Figs. S5-S47).

As a result, the lithic artifacts were not homogeneously distributed. Some areas were quite empty, and it is clear, even at a first glance to the map (Fig. 21, kernel density), that the density of the lithic items differs between the two sides of the skeleton. The artifacts were especially numerous in the proximity of the anterior side of the elephant which probably was the side freed from the mud in which the animal was trapped.

In this area, two major concentrations are evident. The first concentration, cluster A (red in Fig. 22), was found in the area of the cranium of the elephant, immediately over the surface of the incisive bone, in the proximity of the insertion of the left tusk (Fig. 23). This cluster contained 32 lithic items accumulated on both sides of the tusk in two groups of seven (west side) and twenty-five (east side) items. The wider group was accumulated in a very small volume ($25 \times 15 \times 7$ cm) with the artifacts lying in contact or at few centimeters of distance from each other. Two of the more complete refittings (RMU 18 SI Figs. S8, S32-S33 and RMU 20 SI Figs.S9, S36-S37) were part of this accumulation.

The second concentration, cluster B (red in Fig. 22), was larger and measured approximately 2 $m^2$. It was located near the right side of the carcass, in the space

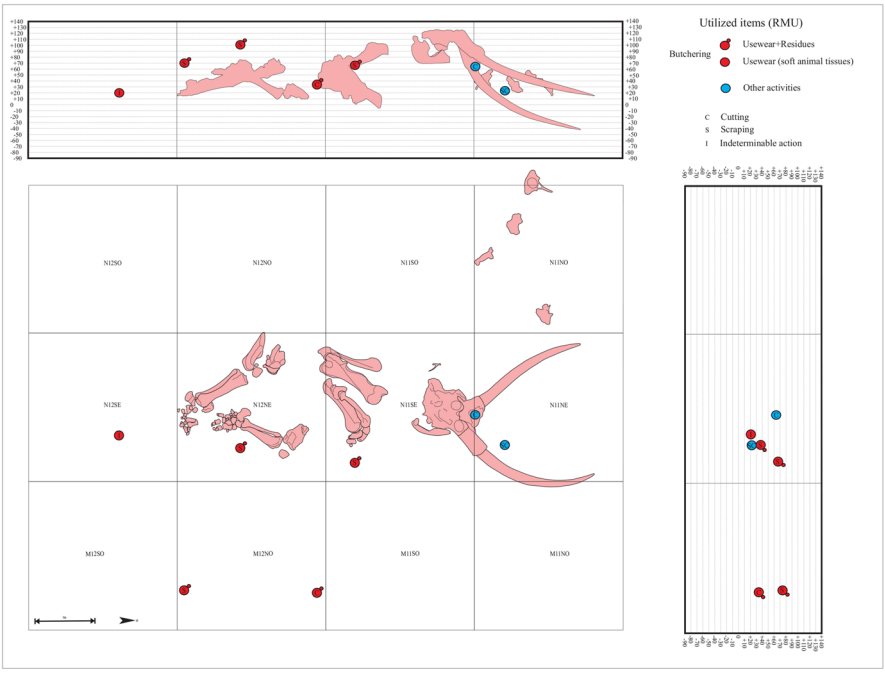


**Fig. 27** Spatial distribution of the used lithic tools pertaining to RMUs

between the foreleg and the skull. Cluster B consisted of 32 lithic items, more than half refit.

Most of the artifacts of both clusters A and B were included in a layer of 20–30 cm in a span of elevations ranging from + 46.5 cm to + 71 cm (cluster A) and from + 33 cm to + 81 cm (cluster B). This span may approximately define a "trampling floor" at the base of the skull and at the level of the joints humerus/radius/ulna. The application of the proximity index (Fig. 22; see also the "Materials and Methods" section) confirmed the reliability of the two clusters.

The proximity analysis allowed us to identify other more peripheral small clusters of few items (generally four or five on average). Some of these small clusters pertained to the same span elevation of the clusters A and B. Other small clusters were positioned at lower elevations (Fig. 22).

To verify possible connections between artifacts and between clusters, the index of proximity, elevation, position, and eventual refitting were extrapolated for each lithic item.

As a result, it was possible to define the spatial relationship between various artifacts and their lines of distribution.

The combination of the clusters A and B with all the artifacts staying in the same elevation span (orange areas and orange spots in Fig. 24) showed an expansion of the two clusters and a discontinuous dispersion on the right side of the carcass, especially oriented southeast. This set of artifacts comprises the 44% of the positioned items, 70% of the artifacts pertaining to the refitting, and 100% of the refitted cores.

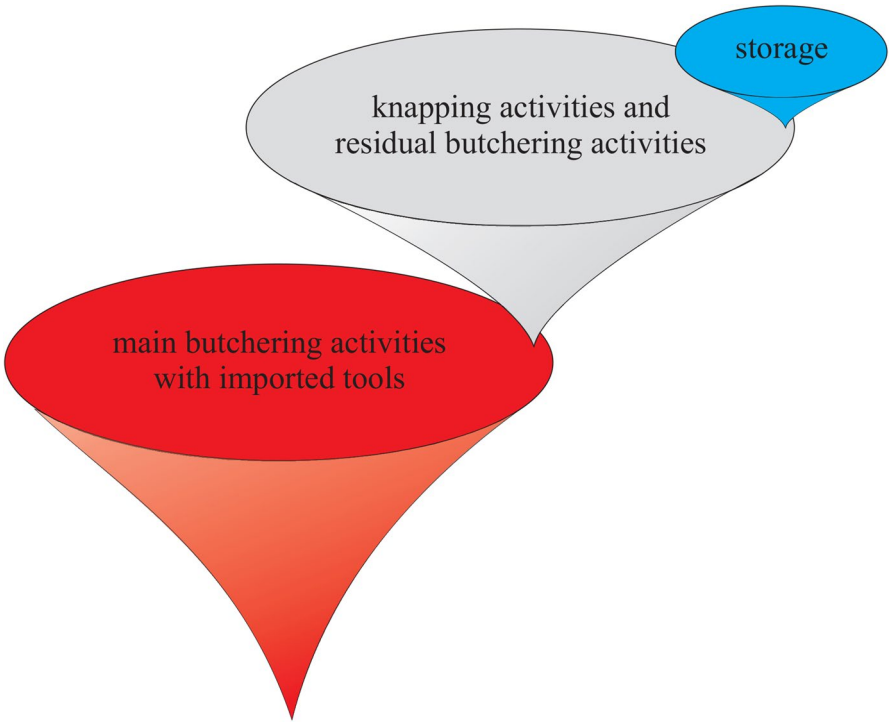


**Fig. 28** Activities and chronology. Small-scale time scan

At lower elevations, various lithic items refit with the RMU were found in the upper span of elevation. As an example, part of the twenty artifacts following the same line of dispersion northwest of the cervical vertebrae of the elephant relate to the refitting RMU 5 (SI Figs.S7, S18-S20) that was scattered around the skull. These data suggest that the lithic artifacts buried in it slipped from the area behind the skull toward lower elevations. Most likely, somehow after the deposition of the lithic artifacts and before the complete burial of the area, the sector

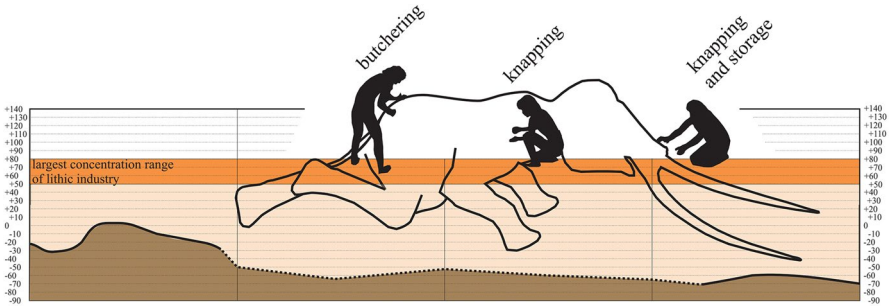


**Fig. 29** Localization of activities around the carcass related to the in loco produced lithic items

northwest underwent some episode of flow, followed by erosion and the localized creation of a difference in height, filled by the slipping of adjacent sediments.

In front of the skull, another line of distribution at lower elevations was recognized. In this area, the progressive lowering of the elevation of the lithic items seems to follow the inclination of the tusks, suggesting a minor episode of sliding. The connection of this line of distribution with cluster B is testified to by the presence of artifacts pertaining to refitting RMUs 7 (SI Figs. S8, 23–249-10) and 14 (Figs. 9–10; SI Fig.S7).

Last, few artifacts laying close to the left backside of the carcass relate mostly to cores located in the southeast line of dispersion, suggesting that the hominins occasionally moved with their tools from the anterior right side of the carcass to the opposite left side.

In the two clusters of major density, the retouched lithic items represented a small percentage (8%) of the lithic items ≥ 1.5 cm. The percentage increased, reaching the 16.5% (1/3 of the total number of retouched items), in the area of dispersion (orange spots on Fig. 24) along the right side of the carcass. At lower heights, near the skull, the right side, and the rear area of the carcass, the retouched tools reached 37% of the lithic items ≥ 1.5 cm (2/3 of all retouched items). On the left side of the carcass, only two flakes roughly retouched were documented.

Regarding the items with use-wear, a density of tools used for processing soft animal tissues was localized on the right side of the carcass near the legs. Items of the cluster B, partly pertaining to the RMUs, and items of the areas in orange on the Fig. 24, were part of this density of tools used for butchering. Another small group of three items used to process wood and medium-hard material were documented in the space between the tusks. They pertained to cluster A and to the dispersion at lower elevation localized in front of the skull. Some of these items pertain to RMUs localized at higher elevation.

## Discussion and Conclusions

The lines of dispersion combined with the results of the refitting analysis show that the lithic items lying on the lower elevations very likely pertained to the trampling floor identified at higher elevations. The spatial analysis allowed us to make visible the taphonomic processes of migration of the lithic tools that occurred in the area, limited to a few meters horizontally and in an interval between a few centimeters to 1 m in height. However, the majority of the RMUs was positioned in a range of 30 cm in height suggesting that only a minimal part of the lithic industry was affected by a notable migration. All the items composing these RMUs fall within this range of 30 cm with few exceptions of single items located at heights slightly lower or higher (see Fig. 1b).

The areas of activities carried out around the elephant may be roughly divided into two blocks. The first block, characterized by butchering and knapping activities, were located on the right side of the animal near the legs. The second block was

localized near the skull of the animal. In this area few lithic tools associated with woodworking were identified; the resulting debitage of knapping activity was also present, accumulated in a pile with other lithic items.

The lithic items recovered in these spaces and the few others lying around the carcass likely represent "mini-palimpsests" resulting from the overlapping of human activities occurring in different stages of decay of the carcass.

During the excavation, layers or surfaces allowing us to document the chronological progression of these activities were not identified. The localization of the lithic items allowed us to distinguish, at least, a small volume of deposit where many refitting events were localized that testifies to a trampling floor. The presence of a volume rather than a surface is due, in addition to human activity, to the natural condition of the deposit and the events occurred on it during syndepositional and postdepositional phases. Intuitively, the plasticity of the tuffite was high when the elephant became stuck in the mud, but we do not know the conditions of the degree of deformation of the trampling floor during the visits of the humans. We can only infer that the sediments reacted differently to the stress of such dissimilar loads and possibly humans exploited the carcass and made the knapping sessions when the sediments were dried.

Moreover, postdepositional disturbances affected the deposit of La Polledrara, influencing the spatial distribution of the lithic items. The variation in saturation occurred at La Polledrara (Marano *et al*., 2021), which probably affected, even if to a lesser extent, the area of the carcass (see the "Site Formation Processes and Degree of Preservation of the Lithic Tools" section), caused the cyclical formation of fissures and percolations from the top of the deposit. It is worth mentioning that the fissures may have caused the displacement downward of some of the lithic items. Moreover, it is also possible that localized dislocation of volumes of deposits occurred as testified to by the line of distribution of the cervical vertebrae of the elephant and by various refitting.

Despite the taphonomic processes documented by the refitting and the spatial analysis, the area of the elephant is doubtless a primary deposit sealed quickly after a few episodes of saturation as indicated by the encrustation of barite detected by SEM–EDX ("Site Formation Processes and Degree of Preservation of the Lithic Tools" section).

The alkaline properties of the barite very likely helped to narrow bacterial proliferation and, thus, to mitigate the decomposition of the residues of organic matter entrapped in the lithic tools. Thus, it was possible to apply residue analysis and to reach positive results despite the antiquity of the site (see also Rots *et al*. (2013); Solodenko *et al*. (2015); Zupancich *et al*. (2016b); Lemorini *et al*. (2020); Venditti *et al*., (2021a, b) for other examples of residue analysis applied to Late Lower Paleolithic sites).

The combination between the residue detected with five independent techniques (morphological, stain, FTIR, PCR, SEM–EDX analyses) and use-wear analysis (Tables 7–8) demonstrates that, at La Polledrara, the fat and meat package guaranteed by the carcass was the material most often processed with the lithic tools.

Lithic tools were rarely in contact with bone. On the retouched flakes ID 20216, 20514, 20635, 20653, bone micro-residues were associated with polish related to soft animal tissues, suggesting episodic contact during butchering activities. Bone scraping detected on the lithic tool ID 20221 may suggest the intention to scrape off the periosteum from fresh bones with the purpose of facilitating its breakage

(Konidaris *et al*., 2018; Venditti *et al*., 2021a, b). BSMs certainly attributable to the contact with lithic cutting edges were not observed on the elephant carcass. The only reliable BSMs were the fracturing marks documented on the diaphysis of the right and left femurs (Cerilli & Fiore, 2018, Fig. 3-1ab, pag.57; Anzidei *et al*., 2021, Fig. 2b, pag.13). A big fragment of leucitite (about 30 cm of maximum dimension) was found close to the right femur (SI Fig. S48). This is the only large stone found in the area of the elephant. Although we cannot demonstrate its link with the fracturing marks, its vicinity to the femur and its angular shape, similar to the shape of tools used for this task in traditional contexts (Haynes et al. 2021) and in experimental sessions (Starkovich *et al*., 2021), may suggest a possible connection.

The processing with the small tools of materials other than animal tissues is almost absent except for two items used for woodworking (ID 20271, 20805) and, in one case, after a previous use for butchering (ID 20271).

Combining the results from residue analysis, use-wear analysis, and spatial analysis, we can reconstruct the interaction between hominins, lithic tools, and the elephant. The spatial analysis documented that the butchering activities were carried out on the right side of the elephant (Figs. 25, 26). The scarce contact of the lithic cutting edges with bone, testified to by the use-wear and by lack of indisputable cut marks on the bones (Anzidei *et al*., 2021; Cerilli & Fiore, 2018), implies that hominins exploited the carcass with the flaked tools when meat was still available, preventing from scraping off dry remains of meat from the bone. Use-wear analysis revealed that various stone tools were used to cut meat suggesting activities focused on stripping off fleshy tissues. In other cases, the stone tools were used in contact with the inner part of the fresh hide. These data seem to suggest that these lithic tools were involved in the deskinning process. Deskinning is the first step of the butchering sequence. In actualist experiments (Gingerich & Stanford, 2018; p. 173 Fig. 5) or modern butchering sessions (Haynes & Klimowicz, 2015; p. 22), sections of hide are cut and pulled back. In Gingerich and Stanford's (2018) paper, the work is cooperatively carried out by two persons, one separating the hide from the meat with a cutting tool and one other person pulling back the hide. Hominins of La Polledrara had probably to remove cooperatively the hide to reach the meat using their lithic tools with a cutting motion. At La Polledrara, fresh hide was processed by cutting and by scraping. Since scraping is unsuitable for removing hide from the carcass, this activity may have a reason only if the aim was to clean up fat and pieces of meat from hide. Thus, we tentatively suggest that the exploitation of the soft tissues of the carcass was characterized by two types of activities, the removal of the meat and the removal of the subcutis fat, carried out in the same or in a shortly delayed chronological span, possibly when the carcass was already devoid of its meat mass.

Besides these activities, the refitting and the spatial analysis documented the production of lithic blanks. Two concentrations corresponding to the clusters A and B testified flintknapping in situ. In these two sets of lithic items, use-wear appears marginal (Fig. 26). Only four out of seven items were used on soft animal tissues; the other three items were used on bone, woodworking, and generic medium hard material. Clusters A and B likely represent two knapping places. The first shows 32 lithic items accumulated in small piles on both sides of the

left tusk and leaning directly on the incisive bone (Fig. 23). Cluster A counts, aside from two of the most complete refitting, isolated items of other refittings and some artifacts not belonging to any of the 28 identified RMUs. The presence of artifacts not pertaining to the in loco refittings at the same height of them and in the same narrow area suggest an intentional accumulation by humans. They probably represented a sort of cache left by the hominins for future uses. Knapping and accumulation events occurred when the carcass was devoid of meat, or almost. This means that the carcass was not only an "organic quarry" (Lemorini, 2018; p.30), a source of meat, fat, and bone raw material. La Polledrara was also a landmark, recognizable by the hominins during their routine back and forth from the area and, thus, possibly used as a cache.

To manage a resource of this type, exploitable in different states of preservation (see also discussion in Venditti *et al*., 2021a, b), a high degree of flexibility was needed. At La Polledrara, this flexibility is testified by the small flakes and small tools used for butchering. Most of them (22 out of 29 items; see the "Refitting" section) do not pertain to the RMUs; they were introduced as single units into the site (Figs. 25, 26). Clearly hominins, during their displacements, were equipped with a ready-use toolkit and with raw material to be knapped on the spot (see also Rocca *et al*., 2021) that, in turn, was probably partly exported as tools of a renovate mobile toolkit.

The site of La Polledrara, similar to other sites in Africa, Europe, and Asia (see Abruzzese and al., 2016; Tourloukis *et al*., 2018; Marinelli *et al*., 2021a and references therein), documents the interaction between lithic items of small size and elephants. The direct link between small tools and the butchering of this animal is testified to, in addition to La Polledrara, by the sites of Marathosa 1 (Tourloukis *et al*., 2018) and Barranc de la Boella (Mosquera *et al*., 2015). The usability of small lithic artifacts to butcher a large animal such as an elephant was recently demonstrated by the experiment conducted by Starkovich *et al*. (2021) on an elephant leg. Nevertheless, the same experiment also testified the difficulties encountered in cutting such a thick mass of hide and meat that, in the past, likely was portioned with the help of other larger lithic or organic tools.

The data obtained from this study and from other published papers (Anzidei *et al*., 2012; Cerilli & Fiore, 2018; Santucci *et al*., 2016) allow us to document that the human-elephant interaction at La Polledrara involved a sequence of events occurring over a long-time span from a fresh carcass to a completely bare skeleton (Fig. 27). The body of the elephant, entrapped in the mud, was the target of butchering sessions occurring in a short time, a few days at most, to exploit the fresh meat. Contemporary or in a delayed time, the carcass was also exploited for its marrow and possibly to obtain bone blanks as the fragmentation of the two femurs testifies (see Sect. 2.1). Then, the skeleton was chosen as a knapping area and as a place to keep flaked lithic items possibly for future use (Figs. 28 and 29). In this interaction, the absence of large carnivores' presences (see for similar cases Rocca *et al*., 2021, and references therein; see for cases with presence of large carnivores Konidaris & Tourloukis, 2021) both as osseous remains and as signs on elephant bones is notable. In the case of La Polledrara, it is possible to speculate that this evidence might be missing due to the lack of some portions of the carcass (see the "The Archaeological Context" section). However, elephant-human-large carnivore interactions are still a puzzle that deserves to be investigated to improve our understanding of the behavior of hominins and their strategies of competition with other predators.

**Supplementary Information** The online version contains supplementary material available at https://doi.org/10.1007/s10816-022-09584-4.

**Acknowledgements** We are deeply indebted with Anna Paola Anzidei† and Anna De Santis of the Soprintendenza Archeologica, Belle Arti e Paesaggio per l'area metropolitana di Roma, who offered us the unique opportunity to study the extraordinary site of La Polledrara.

This article is dedicated to the beloved memory of A.P. Anzidei, whose tenacity and perseverance allowed to promote the uniqueness of the site of La Polledrara di Cecanibbio with a rigorous scientific approach and to offer to the public an extraordinary example of dissemination.

**Author Contribution** C.L. conceptualization; data curation; investigation; methodology; supervision; writing—original draft; writing – review & editing.

E.S. investigation; methodology; supervision; writing—original draft; writing—review and editing.

I.C. investigation; methodology; writing—original draft; writing—review and editing.

A.N. investigation; methodology; writing—original draft; writing—review and editing.

S.N.-C. investigation; methodology; writing—original draft; writing—review and editing.

**Funding** Open access funding provided by Università degli Studi di Roma La Sapienza within the CRUI-CARE Agreement.



## References

Abruzzese, C., Aureli, D., & Rocca, R. (2016). Assessment of the Acheulean in Southern Italy: New study on the Atella site (Basilicata, Italy). *Quaternary International, 393*, 158–168. https://doi.org/10.1016/j.quaint.2015.06.005

Agam, A., & Barkai, R. (2018). Elephant and mammoth hunting during the Paleolithic: A review of the relevant archaeological, ethnographic and ethno-historical records. *Quaternary, 1*(3), 1–28. https://doi.org/10.3390/quat1010003

Anzidei, A. P., Bulgarelli, G. M., Catalano, P., Cerilli, E., Gallotti, R., Lemorini, C., Milli, S., Palombo, M. R., Pantano, W., & Santucci, E. (2012). Ongoing research at the late Middle Pleistocene site of La Polledrara di Cecanibbio (central Italy), with emphasis on human-elephant relationships. *Quaternay International, 255*, 171–187. https://doi.org/10.1016/j.quaint.2011.06.005

Anzidei, A. P., Bulgarelli, G., Cerilli, E., Fiore, I., Lemorini, C., Marano, F., Palombo, M. R. & Santucci, E. (2021). Strategie di sussistenza nel Paleolitico inferiore a La Polledrara di Cecanibbio (Roma): lo sfruttamento di una carcassa di Palaeoloxodon antiquus. In: I. Damiani, A. Cazzella, V. Copat (Eds.), *La preistoria del cibo. L'alimentazione nella preistoria e nella protostoria*. Studi di Preistoria e Protostoria 6 (pp 1–13). Firenze.

Aranguren, B., Grimaldi, S., Benvenuti, M., Capalbo, C., Cavanna, F., Cavulli, F., Ciani, F., Comencini, G., Giuliani, C., Grandinetti, G., Mariotti Lippi, M., Masini, F., Mazza, P. P. A., Pallecchi, P., Santaniello, F., Savorelli, A., & Revedin, A. (2019). Poggetti Vecchi (Tuscany, Italy): A late Middle Pleistocene case of human–elephant interaction. *Journal of Human Evolution, 133*, 32–60. https://doi.org/10.1016/j.jhevol.2019.05.013

Asryan, L., Ollé, A., & Moloney, N. (2014). Reality and confusion in the recognition of post-depositional alterations and use-wear: An experimental approach on basalt tools. *Journal of Lithic Studies, 1*(1), 9–32. https://doi.org/10.2218/jls.v1i1.815

Aureli, D., Contardi, A., Giaccio, B., Jicha, B., Lemorini, C., Madonna, S., Magri, D., Marano, F., Milli, S., Modesti, V., Palombo, M. R., & Rocca, R. (2015). Palaeoloxodon and human interaction: Depositional setting, chronology and archaeology at the Middle Pleistocene Ficoncella site (Tarquinia, Italy). *PLOS ONE, 10*(4). https://doi.org/10.1371/journal.pone.0124498.

Bahl, S., Suwas, S., & Chatterjee, K. (2014). The importance of crystallographic texture in the use of titanium as an orthopedic biomaterial". *The Royal Society of Chemistry Advances, 4*(2), 38078–38087. https://doi.org/10.1039/C4RA05440G

Barkai, R. (2021). The elephant in the Handaxe: Lower Palaeolithic ontologies and representations. *Cambridge Archaeological Journal, 31*(2), 349–361. https://doi.org/10.1017/S0959774320000360

Ben-Dor, M., Gopher, A., Hershkovitz, I., & Barkai, R. (2011). Man the fat hunter: The demise of homo erectus and the emergence of a new hominin lineage in the Middle Pleistocene (ca. 400 kyr) Levant. *PLOS ONE, 6*(12), e28689. https://doi.org/10.1371/journal.pone.0028689

Boëda, E., Geneste, J.-M., & Meignen, L. (1990). Identification des chaînes opératoires du Paléolithique ancien et moyen. *Paleo, 2*, 43–80.

Bordes, F., & Vaufray, R. (1961). *Typologie du Paléolithique ancien et moyen*. Publications de l'Institut de préhistoire de l'Université de Bordeaux 1.

Caporaletti, F., Carbonaro, M., Maselli, P., & Nucara, A. (2017). Hydrogen-Deuterium exchange kinetics in β-lactoglobulin (−)-epicatechin complexes studied by FTIR spectroscopy. *International Journal of Biological Macromolecules, 104*, 521–526. https://doi.org/10.1016/j.ijbiomac.2017.06.028

Caricola, I., Charles, A., Tirillò, J., Charlton, F., Barton, H., Breglia, F., Rossi, A., Deflorian, M. C., De Marinis, A. M., Harris, S., Pellegrini, A., Sacchetti, F., Boccuccia, P., Miari, M., & Dolfini, A. (2022). Organic residue analysis reveals the function of Bronze Age metal daggers. *Scientific Reports, 12*, 6101. https://doi.org/10.1038/s41598-022-09983-3

Castorina, F., Masi, U., Milli, S., Anzidei, A. P., & Bulgarelli, G. M. (2015). Geochemical and Sr-Nd isotopic characterization of Middle Pleistocene sediments from the paleontological site of La Polledrara di Cecanibbio (Sabatini Volcanic District, central Italy). *Quaternary International, 357*, 253–263. https://doi.org/10.1016/j.quaint.2014.04.004

Cerilli, E, & Fiore, I. (2018). Natural and anthropic events at La Polledrara di Cecanibbio (Italy, Rome): Some significant examples. *Alpine and Mediterranean Quaternary, 31* (Quaternary: Past, Present, Future - AIQUA Conference, Florence, 13–14/06/2018), 55 – 58.

Chan, B., Gibaja, J. F., García-Díaz, V., Hoggard, C. S., Mazzucco, N., Rowland, J. T., & van Gijn, A. L. (2020). Towards an understanding of retouch flakes: A use-wear blind test on knapped stone microdebitage. *PLoS ONE, 15*(12), e0243101. https://doi.org/10.1371/journal.pone.0243101

Chazan, M. (2013). Butchering with small tools: The implications of the Evron Quarry assemblage for the behaviour of Homo erectus. *Antiquity, 87*, 350–367. https://doi.org/10.1017/S0003598X00048997

Crabtree, D. E. (1972). *An introduction to flint knapping*. Idaho State University Museum.

Cziesla, E. (1990). On refitting of stone artefacts. In E. Cziesla, S. Eickhoff, N. Arts, & D. Winter (Eds.), *The Big Puzzle: international symposium on refitting stone artefacts* (pp. 9–44). Holos, Bonn: Studies in Modern Archaeology.

de la Peña, P. (2015). The interpretation of bipolar knapping in African Stone Age Studies. *Current Anthropology, 56*(6), 911–923. https://doi.org/10.1086/684071

Ellingham, S. T. D., Thompson, T. J. U., & Islam, M. (2017). Scanning electron microscopy–energy-dispersive X-ray (SEM/EDX): A rapid diagnostic tool to aid the identification of burnt bone and contested cremains. *Journal of Forensic Science, 63*(2), 504–510. https://doi.org/10.1111/1556-4029.13541

Faivre, J.-P., Geneste, J.-M., & Turq, A.(2011). La fracturation en *Split*, une technique de production dans l'industrie lithique des Tares (Sourzac, Dordogne). In In V.Mourre, & M.Jarry (Eds), Entre le marteau et l'enclume: La percussion directe au percuteur dur et la diversité de ses modalités *d'application* (Actes de la table ronde de Toulouse 15–17 mars 2004, pp. 133–142). PALEO 2009–2010, numéro spécial.

Forbes, S. L., Stuart, B. H., Dadour, I. R., & Dent, B. B. (2004). A preliminary investigation of the stages of adipocere formation. *Journal of Forensic Science, 49*(3), 566–574. PMID: 15171178.

Frahm, E., Adler, D. S., Gasparyan, B., Luo, B., Mallol, C., Pajović, G., Gilbert, B., Tostevin, G. T., Yeritsyan, B., & Monnier, G. (2022). Every contact leaves a trace: Documenting contamination in lithic residue studies at the Middle Palaeolithic sites of Lusakert Cave 1 (Armenia) and Crvena Stijena (Montenegro). *PLoS ONE, 17*(4), e0266362. https://doi.org/10.1371/journal.pone.0266362

Fullagar, R., Stephenson, B., & Hayes, E. (2017). Grinding grounds: Function and distribution of grinding stones from an open site in the Pilbara, western Australia. *Quaternary International, 427*, 175–183.

Funiciello, R. & Giordano, G. (Eds), (2008). *Note Illustrative della carta geologica d'Italia, alla scala 1:50.000, foglio 374 Roma*. Firenze, pp. 31-33.

Gingerich, J. A. M., & Stanford, D. J. (2018). Lessons from Ginsberg: An analysis of elephant butchery tools. *Quaternary International, 466*, 269–283. https://doi.org/10.1016/j.quaint.2016.03.025

Gremlich, H. U., & Bing, Y. (Eds.). (2001). *Infrared and Raman spectroscopy of biological materials*. CRC Press.

Gröning, K., & Saller, M. (2000). *L'elefante. Tra natura e cultura* (italian edition). Könemann ed. Köln.

Habuda-Stanić, M., Ravančić, M., & Flanagan, A. (2014). A review on adsorption of fluoride from aqueous solution. *Materials, 7*(9), 6317–6366. https://doi.org/10.3390/ma7096317

Hayes, E., & Rots, V. (2019). Documenting scarce and fragmented residues on stone tools: An experimental approach using optical microscopy and SEM-EDS. *Archeological and Anthropological Science, 11*(7), 3065–3099. https://doi.org/10.1007/s12520-018-0736-1

Haynes, G., & Krasinski, K. (2021). Butchering marks on bones of Loxodonta africana (African savanna elephant): Implications for interpreting marks on fossil proboscidean bones. *Journal of Archaeological Science: Reports, 37*. https://doi.org/10.1016/j.jasrep.2021.102957

Haynes, G., & Klimowicz, J. (2015). Recent elephant-carcass utilization as a basis for interpreting mammoth exploitation. *Quaternary International, 359–360*, 19–37. https://doi.org/10.1016/j.quaint.2013.12.040

Inizan, M. L., Reduron, M., Roche, H., & Tixier, J. (1995). *Technologie de la pierre taillee*. Meudon: C.R.E.P. p.79.Editions du CREP, Meudon.

Key, A. J., & Lycett, S. J. (2015). Edge angle as a variably influential factor in flake cutting efficiency: An experimental investigation of its relationship with tool size and loading. *Archaeometry, 57*(5), 911–927.

Konidaris, G., & Tourloukis, V. (2021). Proboscidea-Homo interactions in open-air localities during the Early and Middle Pleistocene of Western Eurasia: A palaeontological and archaeological perspective. In G. Konidaris, R. Barkai, V. Tourloukis, & K. Harvati (Eds.), *Human-elephant interactions: From past to present* (pp. 67–104). Tübingen University Press.

Konidaris, G. E., Athanassiou, A., Tourloukis, V., Thompson, N., Giusti, D., Panagopoulou, E., & Harvati, K. (2018). The skeleton of a straight-tusked elephant (Palaeoloxodon antiquus) and other large mammals from the Middle Pleistocene butchering locality Marathousa 1 (Megalopolis Basin, Greece): Preliminary results. *Quaternary International, 497*, 65–84. https://doi.org/10.1016/j.quaint.2017.12.001

Lemorini, C., Cristiani, E., Cesaro, S., Venditti, F., Zupancich, A., & Gopher, A. (2020). The use of ash at Late Lower Paleolithic Qesem Cave, Israel—An integrated study of use-wear and residue analysis. *PLoS ONE, 15*(9), e0237502. https://doi.org/10.1371/journal.pone.0237502

Lemorini, C. (2018). Small Tools and the Palaeoloxodon - Homo interaction in the Lower Palaeolithic: The contribution of use-wear analysis. In V. Borgia, & E. Cristiani (Eds), *Palaeolithic Italy. Advanced studies on early human adaptations in the Apennine peninsula*.(pp. 27–36). Sidestone Press, Leiden.

Lombard, M., & Wadley, L. (2007). The morphological identification of micro-residues on stone tools using light microscopy: Progress and difficulties based on blind tests. *Journal of Archaeological Science, 34*(1), 155–165. https://doi.org/10.1016/j.jas.2006.04.008

Marano, F., Palombo, M. R., Cerilli, E., & Milli, S. (2021). The fossilization of mammal bones at La Polledrara Di Cecanibbio (Rome, Central Italy). Insights for in situ Preservation. *Alpine and Mediterranean Quaternary, 34*(1), 1–16.

Marinelli, F., Lemorini, C., & Barkai, R. (2021a). Lower Palaeolithic small flakes and megafauna: The contribution of experimental approach and use-wear analysis to reveal the Link (Chapter 8). In G. E. Konidaris, R. Barkai, R., V. Tourloukis, & K. Harvati (Eds.), *Human-elephant interactions: from past to present*. (pp. 237–260).Tübingen University Press, Tübingen. https://doi.org/10.15496/publikation-55604.

Marinelli F., Lemorini, C., & Barkai, R. (2021b). Experimental archaeology for the interpretation of use-wear. The case study of the small tools of Fontana Ranuccio (late Lower Palaeolithic, Central Italy). In S.Beyries, C.Hamon, Y.Maigrot (Eds), *Beyond Use-Wear Traces: Going from tools to people by means of archaeological wear and residue analyses (*pp. 117–128). Sidestone Press, Leiden.

Martín-Viveros, J. I., & Ollé, A. (2020). Use-wear and residue mapping on experimental chert tools. A multi-scalar approach combining digital 3D, optical, and scanning electron microscopy. *Journal of Archaeological Science: Reports, 30*, 102236. https://doi.org/10.1016/j.jasrep.2020.102236

Milli, S., & Palombo, M. R. (2005). The high-resolution sequence stratigraphy and the mammal fossil record: A test in the Middle-Upper Pleistocene deposits of the Roman Basin (Latium, Italy). *Quaternary International, 126e128*, 251e270. https://doi.org/10.1016/j.quaint.2004.04.025

Milli, S., Moscatelli, M., Palombo, M. R., Parlagreco, L., & Paciucci, M. (2008). Incised-valleys, their filling and mammal fossil record: An example in the Middle-Upper Pleistocene deposits of the Roman Basin (Latium, Italy). *Geoacta, Special Publication, 1*, 67e88.

Mosquera, M., Saladié, P., Ollé, A., Cáceres, I., Huguet, R., Villalaín, J. J., Carrancho, A., Bourlès, D., Braucher, R., & Vallverdú, J. (2015). Barranc de la Boella (Catalonia, Spain): An Acheulean elephant butchering site from the European late Early Pleistocene. *Journal of Quaternary Science, 30*(7), 651–666. https://doi.org/10.1002/jqs.2800

Nucara, A., Nunziante-Cesaro, S., Venditti, F., & Lemorini, C. (2020). A multivariate analysis for enhancing the interpretation of infrared spectra of plant residues on lithic artefacts. *Journal of Archaeological Science Reports, 33*.https://doi.org/10.1016/j.jasrep.2020.102526

Panagopoulou, E., Tourloukis, V., Thompson, N., Konidaris, G., Athanassiou, A., Giusti, D., Tsartsidou, G., Karkanas, P., & Harvati, K. (2018). The Lower Palaeolithic site of Marathousa 1, Megalopolis, Greece: Overview of the evidence. *Quaternary International, 497*, 33–46. https://doi.org/10.1016/j.quaint.2018.06.031

Pargeter, J., & Eren, M. I. (2017). Quantifying and comparing bipolar versus freehand flake morphologies, production currencies, and reduction energetics during lithic miniaturization. *Lithic Technology, 42*, 90–108. https://doi.org/10.1080/01977261.2017.1345442

Pargeter, J., & Shea, J. J. (2019). Going big versus going small: Lithic miniaturization in hominin lithic technology. *Evolutionary Anthropology, 28*, 72–85. https://doi.org/10.1002/evan.21775

Pedergnana, A. (2020). "All that glitters is not gold": Evaluating the nature of the relationship between Archeological residues and stone tool function. *Journal of Paleolithic Archeology, 3*(3), 225–254.

Perdegnana, A., & Ollè, A. (2018). Building an experimental comparative reference collection for lithic micro-residue analysis based on a multi-analytical approach. *Journal of Archaeological Method and Theory, 25*(1), 117–154. https://doi.org/10.1007/s10816-017-9337-z

Pedergnana, A., Asryan, L., Fernández-Marchena, J. L., & Ollé, A. (2016). Modern contaminants affecting microscopic residue analysis on stone tools: A word of caution. *Micron, 86*, 1–21. https://doi.org/10.1016/j.micron.2016.04.003

Pereira, A., Nomade, S., Falguères, C., Bahain, J. J., Tombret, O., Garcia, T., Voinchet, P., Bulgarelli, M. G., & Anzidei, A. P. (2017). 40Ar/39Ar and ESR/U-series data for the La Polledrara di Cecanibbio archaeological site (Lazio, Italy). *Journal of Archaeological Science: Reports, 15*, 20–29. https://doi.org/10.1016/j.jasrep.2017.05.025

Reshef, H., & Barkai, R. (2015). A taste of an elephant: The probable role of elephant meat in Paleolithic diet preferences. *Quaternary International, 379*, 28–34. https://doi.org/10.1016/j.quaint.2015.06.002

Rocca, R., Boshin, F., & Aureli, D. (2021). Around an elephant carcass: Cimitero di Atella and Ficoncella in the behavioural variability during the early Middle Pleistocene in Italy (Chapter 10). In G. E. Konidaris, R. Barkai, V. Tourloukis, & K. Harvati (Eds.), *Human-elephant interactions: from past to present* (pp. 287–302). Tübingen: Tübingen University Press. https://doi.org/10.15496/publikation-55604

Roebroeks, W. (1988). *From find scatters to early hominid behaviour: A study of middle Paleolithic riverside settlements at Maastricht-Belvedere (The Netherlands)*. Leiden: Analecta Praehistorica Leidensia 21.

Romagnoli, F., & Vaquero, M. (2019). The challenges of applying refitting analysis in the Palaeolithic archaeology of the twenty-first century: An actualised overview and future perspectives. *Archaeological and Anthropological Science, 11*, 4387–4396. https://doi.org/10.1007/s12520-019-00888-3

Rots, V. (2010). *Prehension and hafting traces on flint tools: A methodology*. Leuven University Press.

Rots, V., Hardy, B. L., Serangeli, J., & Conard, N. J. (2013). Residue and microwear analyses of the stone artifacts from Schöningen. *Journal of Human Evolution, 89*, 298–308. https://doi.org/10.1016/j.jhevol.2015.07.005

Santucci, E., Marano, F., Cerilli, E., Fiore, I., Lemorini, C., Palombo, M. R., Anzidei, A. P., & Bulgarelli, G. M. (2016). Palaeoloxodon exploitation at the Middle Pleistocene site of La Polledrara di Cecanibbio (Rome, Italy). *Quaternary International, 406*, 169–182. https://doi.org/10.1016/j.quaint.2015.08.042

Solodenko, N., Zupancich, A., Cesaro, S. N., Marder, O., Lemorini, C., & Barkai, R. (2015). Fat residue use-wear found on Acheulian biface scraper associated with butchered elephant remains at the site of Revadim, Israel. *PLOS ONE, 1* (3). https://doi.org/10.1371/journal.pone.0118572.

Starkovich, B. M., Cuthbertson, P., Kitagawa, K., Thompson, N., Konidaris, G. E., Rots, R., Münzel, S. C., Giusti, D., Schmid, V. C., Blanco-Lapaz, A., Lepers, C., & Tourloukis, V. (2021). Minimal tools, maximum meat: A pilot experiment to butcher an elephant foot and make elephant bone tools using

lower Paleolithic stone tool technology. *Ethnoarchaeology, 12*(2), 118–147. https://doi.org/10.1080/19442890.2020.1864877

Stephenson, B. (2015). A modified Picro-Sirius Red (PSR) staining procedure with polarization microscopy for identifying collagen in archaeological residues. *Journal of Archaeological Science, 61*, 235–243. https://doi.org/10.1016/j.jas.2015.06.007

Tironia, A., Trezza, M. A., Irassara, E. F., & Scian, A. N. (2012). Thermal treatment of kaolin: Effect on the pozzolanic activity. *Procedia Materials Science, 1*, 343–350. https://doi.org/10.1016/j.mspro.2012.06.046

Todeschini, R. (1998). *Introduzione alla Chemiometria*. Edises.

Tourloukis, V., Thompson, N., Panagopoulou, E., Giusti, D., Konidaris, G. E., Karkanas, P., & Harvati, K. (2018). Lithic artifacts and bone tools from the Lower Palaeolithic site Marathousa 1, Megalopolis, Greece: Preliminary results. *Quaternary International, 497*, 47–64. https://doi.org/10.1016/j.quaint.2018.05.043

Venditti, F., Agam, A., Tirillò, J., Nunziante- Cesaro, S., & Barkai, R. (2021a). An integrated study discloses chopping tools use from Late Acheulean Revadim (Israel). *PLoS ONE, 16*(1), e0245595. https://doi.org/10.1371/journal.pone.0245595

Venditti, F., Agam, A., Tirillo, J., Nunziante-Cesaro, S., & Barkai, R. (2021b). An integrated study discloses chopping tools use from Late Acheulean Revadim (Israel). *PLoS ONE, 16*(1), e0245595. https://doi.org/10.1371/journal.pone.0245595

Wadley, L., Lombard, M., & Williamson, B. (2004). The first residue analysis blind tests: Results and lessons learnt. *Journal of Archaeological Science, 31*(11), 1491–1501.

White, P. A., & Diedrich, C. G. (2012). Taphonomy story of a modern African elephant Loxodonta africana carcass on a lakeshore in Zambia (Africa). *Quaternary International, 276–277*, 287–296. https://doi.org/10.1016/j.quaint.2012.07.025

Wright, K. (2017). The NIPALS algorithm. https://cran.rproject.org/web/packages/nipals/vignettes/nipals_algorithm.html

Zupancich, A., Lemorini, C., Gopher, A., & Barkai, R. (2016a). On Quina and demi-Quina scraper handling: Preliminary results from the late Lower Paleolithic site of Qesem Cave, Israel. *Quaternary International, 398*, 94–102. https://doi.org/10.1016/j.quaint.2015.10.101

Zupancich, A., Nunziante-Cesaro, S., Blasco, R., Rosell, J., Cristiani, E., Venditti, F., Lemorini, C., Barkai, R., & Gopher, A. (2016b). Early evidence of stone tool use in bone working activities at Qesem Cave, Israel. *Scientific Reports, 6*, 37686. https://doi.org/10.1038/srep37686

Zutovski, K., & Barkai, R. (2016). The use of elephant bones for making Acheulian handaxes: A fresh look at old bones. *Quaternary International, 406*, 227–238. https://doi.org/10.1016/j.quaint.2015.01.033



## Authors and Affiliations

**Cristina Lemorini[1] · Ernesto Santucci[2] · Isabella Caricola[1] · Alessandro Nucara[3] · Stella Nunziante-Cesaro[4]**

[1] LTFAPA Laboratory, Department of Science of Antiquities, Sapienza University of Rome, Italy, P.le A.Moro 5, Rome 00185, Italy

[2] Sen.Piacentini 12, Rieti, Collevecchio 02042, Italy

[3] Department of Physics, "Sapienza" University of Rome, P.le A.Moro 5, 00185 Rome, Italy

[4] Scientific Methodologies Applied to Cultural Heritage (SMATCH), Largo U.Bartolomei 5, 00136 Rome, Italy